



# International CI Summer School 2015

## Short Course on *Reactive Flow Modelling*

Fabrizio Bisetti | May 29, 2015

CLEAN COMBUSTION RESEARCH CENTER



# Overview



## Topics

- Transport equations
- Software tools
- Thermodynamics
- Transport
- Kinetics
- Stoichiometry
- Laminar premixed flames
- Laminar nonpremixed flames
- Zero-dimensional reactors
- Low mach number approach



# Transport equations

# The momentum equation



The momentum equation for a variable density, variable properties ( $\mu$ ), Newtonian fluid reads as follows:

$$\rho \frac{D\mathbf{u}}{Dt} = -\nabla p + \nabla \cdot \mu \left( \nabla \mathbf{u} + \nabla \mathbf{u}^T - \frac{2}{3}(\nabla \cdot \mathbf{u})\mathbf{I} \right) \quad (1)$$

In the equation above:

- The equation is a vector equation for the three components
- The operators are specific to coordinate systems (Cartesian, cylindrical, polar, etc.): see Appendix in Batchelor's book for examples.
- The convective term is  $\mathbf{u}\nabla\mathbf{u}$
- The material derivative is defined as  $D/Dt = \partial/\partial t + \mathbf{u}\nabla$

# Species mass conservation



We begin from the transport equation for  $\rho_i = \rho Y_i$ ,  
the mass fraction of species  $i$  (e.g. Williams, 1994, p. 2).

$$\boxed{\frac{\partial \rho_i}{\partial t} + \nabla \rho_i \mathbf{v}_i = \dot{\omega}_i} \quad (2)$$

where  $\rho_i \mathbf{v}_i$  is the mass flux of species  $i$  ( $\text{kg}/\text{m}^3\text{-s}$ ).

Define the velocity  $\mathbf{v}_i$  as the sum of two components: the “mass-averaged” bulk velocity  $\mathbf{u}$  and the “diffusion velocity”  $\mathbf{V}_i$ :

$$\mathbf{v}_i = \mathbf{V}_i + \mathbf{u} \quad \text{where} \quad \mathbf{u} = \sum_{i=1}^K Y_i \mathbf{v}_i \quad (3)$$

Note that, since  $\sum Y_i = 1$  by definition of mass fractions, one obtains the result

$$\boxed{\sum_{i=1}^K Y_i \mathbf{v}_i = 0} \quad (4)$$

# Mass conservation



Equation (2) may be summed over all species to recover the continuity equation,

$$\sum_{i=1}^K \frac{\partial \rho_i}{\partial t} + \nabla \rho_i \cdot \mathbf{v}_i = \dot{\omega}_i \quad (5)$$

$$\frac{\partial \rho}{\partial t} + \nabla \rho \cdot \mathbf{u} = - \sum_{i=1}^K \nabla \cdot (\rho Y_i \mathbf{v}_i) + \sum_{i=1}^K \dot{\omega}_i \quad (6)$$

$$\frac{\partial \rho}{\partial t} + \nabla \rho \cdot \mathbf{u} = - \nabla \cdot \left( \rho \sum_{i=1}^K Y_i \mathbf{v}_i \right) + \sum_{i=1}^K \dot{\omega}_i = 0 \quad (7)$$

This result has important computational implications as it illustrates that

*"The conservation equations for the mass fractions of individual species maintain consistency with the continuity equation by virtue of the definition of the diffusion velocities"*

# Closures for diffusion velocities



Let us now write the conservation equations for the density of species  $i$

$$\rho \frac{DY_i}{Dt} = \rho \frac{\partial Y_i}{\partial t} + \rho \mathbf{u} \nabla Y_i = \frac{\partial \rho Y_i}{\partial t} + \nabla \cdot (\rho Y_i \mathbf{u}) = -\nabla \cdot (\rho Y_i \mathbf{v}_i) + \dot{\omega}_i, \quad (8)$$

It is clear that we need a closure for the diffusion velocity  $\mathbf{v}_i$  and that the closure needs to be consistent with the constraint  $\sum Y_i \mathbf{v}_i = 0$ .

There exist a handful of closure options for  $\mathbf{v}_i$ , which are used in practical numerical combustion codes:

- Maxwell-Stefan equations
- Fick's law
- Constant Lewis number
- Hirschfelder & Curtiss approximation

# The Maxwell-Stefan equations



If the contributions of pressure, body forces, and Soret effect are neglected, the diffusion velocities  $\mathbf{V}_i$  obey the Maxwell<sup>1</sup>-Stefan<sup>2</sup>equations (e.g. Bird et al., 2007, p. 538):

$$\nabla X_i = \sum_{j=1}^K \frac{X_i X_j}{D_{ij}} (\mathbf{V}_i - \mathbf{V}_j) \quad (9)$$

where  $X_i$  is the mole fraction of species  $i$  and  $D_{ij}$  are the *binary* diffusivities calculated utilizing the Chapman-Enskog kinetic theory (e.g. Bird et al., 2007, pp. 526–527).

*"The Maxwell-Stefan equations provide the most accurate description of mass transport".*

---

<sup>1</sup>James Clerk Maxwell (13 June 1831 - 5 November 1879) was a Scottish scientist in the field of mathematical physics.

<sup>2</sup>Joseph Stefan (24 March 1835 - 7 January 1893) was a Slovene physicist, mathematician, and poet of the Austrian Empire.

# Computational implications



The Maxwell-Stefan equations have important computational implications that can be understood easily if the equations are recast as a linear system for the 3 components of each species' diffusion velocity:  $(V_{i,x}, V_{i,y}, V_{i,z})$  ( $i = 1, \dots, K$ ).

E.g., consider a system of 3 components, then one has 3 **vector** equations

$$\begin{vmatrix} \frac{X_1 X_2}{D_{12}} + \frac{X_1 X_3}{D_{13}} & -\frac{X_1 X_2}{D_{12}} & -\frac{X_1 X_3}{D_{13}} \\ -\frac{X_1 X_2}{D_{12}} & \frac{X_1 X_2}{D_{12}} + \frac{X_2 X_3}{D_{23}} & -\frac{X_2 X_3}{D_{23}} \\ -\frac{X_1 X_3}{D_{13}} & -\frac{X_2 X_3}{D_{23}} & \frac{X_1 X_3}{D_{13}} + \frac{X_2 X_3}{D_{23}} \end{vmatrix} \begin{vmatrix} \mathbf{V}_1 \\ \mathbf{V}_2 \\ \mathbf{V}_3 \end{vmatrix} = \begin{vmatrix} \nabla X_1 \\ \nabla X_2 \\ \nabla X_3 \end{vmatrix} \quad (10)$$

For an ensemble of  $K$  species, the solution of the system of  $3K$  equations in  $3K$  unknowns is required **at each grid point, every time** the gradients and/or the mole fractions vary.

# Some perspectives...



Recall that with direct methods, the cost of solving linear systems scales as  $\mathcal{O}(N^3)$ , where  $N$  is the number of unknowns.

*"The computational cost of using the Maxwell-Stefan equations to describe mass transport is impractical for all, except the simplest problems, e.g., 1D flames of small molecule fuels that may be described with a small number of species".*

# A radical assumption leading to Fick's law: $\mathcal{D}_{ij} = \mathcal{D}$



If we now set  $\mathcal{D}_{ij} = \mathcal{D}$ , i.e. all binary diffusivities are equal, it can be shown (e.g. Williams, 1994, pp. 10–11) that the Maxwell-Stefan equations (Eq. (9)) reduce to Fick's law for each species:

$$\mathbf{V}_i = -\mathcal{D} \ln \nabla Y_i = -\mathcal{D} \frac{\nabla Y_i}{Y_i}. \quad (11)$$

Upon substituting Eq. (11) into Eq. (8), we obtain

$$\rho \frac{DY_i}{Dt} = \nabla \cdot (\rho \mathcal{D} \nabla Y_i) + \dot{\omega}_i \quad (12)$$

Equation (12) is valid under the following assumptions: (1) Neglect mass transport due to  $\nabla p/p$ ; (2) All species experience the same body force, e.g. gravity; (3) Neglect Soret effects; and (4)  $\mathcal{D}_{ij} = \mathcal{D}$ .

The closure for  $\mathbf{V}_i$  shown in Eq. (11) is consistent with the continuity equation as it is obvious that  $\sum Y_i \mathbf{V}_i = -\sum \mathcal{D} \nabla Y_i = -\mathcal{D} \nabla \sum Y_i = 0$ .

# Hirschfelder and Curtiss approximation



The rigorous solution of the system in Eq. (9) is often replaced by the Hirschfelder and Curtiss approximation (e.g. Poinsot and Veynante, 2005, p. 14):

$$\mathbf{v}_i X_i = -\mathcal{D}_i \nabla X_i, \quad (13)$$

$$\mathcal{D}_i = \frac{1 - Y_i}{\sum_{j \neq i} X_j / \mathcal{D}_{ij}}. \quad (14)$$

If this approximation is used, the diffusive flux becomes:

$$\rho Y_i \mathbf{v}_i = -\rho \mathcal{D}_i \frac{Y_i}{X_i} \nabla X_i = -\rho \mathcal{D}_i \frac{\nabla(W Y_i)}{W}. = -\rho \mathcal{D}_i Y_i \frac{\nabla W}{W} - \rho \mathcal{D}_i \nabla Y_i. \quad (15)$$

Note that in addition to the “Fickian” term  $\nabla Y_i$ , there is a second term related to gradients of the mixture-averaged molar mass  $W$ , which is often neglected (or simply “forgotten” by mistake).

# Constant Lewis number



A related simplification is possible by letting  $\mathcal{D}_i = \mathcal{D}/\text{Le}_i$ , where  $\lambda = \rho \mathcal{D} C_p$  is the thermal conductivity of the mixture and  $\text{Le}_i$  is the species' Lewis number.

$$\rho Y_i \mathbf{v}_i = -\rho \mathcal{D}_i \frac{Y_i}{X_i} \nabla X_i = -\frac{\rho \mathcal{D}}{\text{Le}_i} Y_i \frac{\nabla W}{W} - \frac{\rho \mathcal{D}}{\text{Le}_i} \nabla Y_i. \quad (16)$$

Note that the Lewis number is kept constant throughout the computational domain. Below a table with a handful of Lewis number values.

H <sub>2</sub> O	1.055	H	0.228
CH <sub>4</sub>	1.260	O	0.906
N <sub>2</sub>	1.436	OH	0.924
CO	1.414	CH <sub>3</sub>	1.271
O <sub>2</sub>	1.424	HCO	1.614
CO <sub>2</sub>	1.737	CH <sub>2</sub> O	1.626

Table: Lewis numbers for selected species as computed at the location of peak heat release rate in a one-dimensional stoichiometric premixed flame at atmospheric pressure.

# Implications for mass conservation



Regardless of the definition of  $\mathcal{D}_i$  (i.e., Hirschfelder & Curtiss or constant Lewis number), Eq. (13) leads to loss of mass conservation since, in general,  
 $\sum Y_i \mathbf{V}_i \neq 0$ .

A widely adopted remedy is to enforce mass conservation by correcting  $\mathbf{u}$  with  $\mathbf{u}^c$ , Eq. (8) becomes:

$$\frac{\partial \rho Y_i}{\partial t} + \nabla \cdot (\rho(\mathbf{u} + \mathbf{u}^c) Y_i) = -\nabla \cdot (\rho Y_i \mathbf{V}_i) + \dot{\omega}_i. \quad (17)$$

Starting from Eq. (13) for  $\mathbf{V}_i$ , the correction velocity is:

$$\mathbf{u}^c = - \sum_{i=1}^K Y_i \mathbf{V}_i = \sum_{i=1}^K \mathcal{D}_i \frac{W_i}{W} \nabla X_i = \sum_{i=1}^K \mathcal{D}_i \frac{\nabla(Y_i W)}{W} \quad (18)$$

$$= \sum_{i=1}^K \mathcal{D}_i Y_i \frac{\nabla W}{W} + \sum_{i=1}^K \mathcal{D}_i \nabla Y_i \quad (19)$$

# Some perspectives and practical aspects of mass conservation



- Adding a correction velocity to a reactive flow solver that uses explicit time integration is rather straightforward. It is less so in the case of an implicit time integration strategy, where  $\mathbf{u}^c$  introduces a direct coupling among convective and diffusive fluxes.
- The expression for the correction velocity is a function of the model used for the diffusive velocity, so that one needs to be careful in actual implementations.
- Mass conservation bears important implications on enthalpy (i.e., energy) conservation, since mass transport implies transport of heat of formation.
- It may be tempting to simply correct the mass fractions to sum to unity periodically during the integration of the reactive Navier-Stokes equations.  
  
This is often a “bad idea” that may lead to unexpected solution behavior, and convergence issues. Further, there are multiple ways to correct the mass fractions (e.g., correct the most abundant species, renormalize all mass fractions, etc.)

# Enthalpy conservation I



Start with the definition of enthalpy per unit mass for a mixture of ideal gases:

$$h(T, Y) = \sum_{i=1}^K h_i(T) Y_i \quad (20)$$

$$\left. \frac{\partial h}{\partial T} \right|_Y = C_p(T, Y) = \sum_{i=1}^K C_{p,i}(T) Y_i \quad (21)$$

The transport equation for the mixture's enthalpy per unit mass  $h$  is (e.g. Bird et al., 2007, p. 589):

$$\boxed{\rho \frac{Dh}{Dt} = -\nabla \cdot \mathbf{q} + \frac{Dp}{Dt}} \quad (22)$$

where external heat sources and viscous heating have been neglected, and it has been assumed that the same external force (e.g. gravity) acts upon all species.

# Enthalpy conservation II



The heat flux  $\mathbf{q}$  for multicomponent mixtures is (e.g. Williams, 1994, p. 5):

$$\mathbf{q} = -\lambda \nabla T + \rho \sum_{i=1}^K h_i(T) Y_i \mathbf{V}_i \quad (23)$$

where the Dufour effect has been neglected.

An important observation with regard to Eq. (22) and Eq. (23) is in order:

*“Consistency between the conservation equations for species and the enthalpy equation, which results in strict energy conservation, is enforced through the proper and consistent definition of the term  $\nabla \mathbf{q}$  and diffusion velocities  $\mathbf{V}_i$ .*

# Enthalpy conservation III



If Fick's law (Eq. (11)) is applied then the flux  $\mathbf{q}$  becomes:

$$\mathbf{q} = -\lambda \nabla T - \rho \mathcal{D} \sum_{i=1}^K h_i(T) \nabla Y_i. \quad (24)$$

Upon substituting Eq. (24) into Eq. (22), we obtain:

$$\rho \frac{Dh}{Dt} = \frac{Dp}{Dt} + \nabla \cdot (\lambda \nabla T) + \nabla \cdot \left( \rho \mathcal{D} \sum_{i=1}^K h_i(T) \nabla Y_i \right). \quad (25)$$

Equation (25) is valid under the following assumptions:

- Let  $\mathcal{D}_{ij} = \mathcal{D}$
- Neglect mass transport due to  $\nabla p/p$ , Soret and Dufour effects
- Neglect viscous heating and external heat sources and assume all species experience the same body force, e.g. gravity

# Enthalpy conservation IV



A last simplification to Eq. (25) is possible if we further assume  $\lambda = \rho \mathcal{D} C_p$  to obtain:

$$\boxed{\frac{Dh}{Dt} = \frac{Dp}{Dt} + \nabla \cdot (\rho \mathcal{D} \nabla h)} \quad (26)$$

which gives a canonical conservation equation for  $h$ .

In closing, we note again that Eq. (26) is a result of a set of simplifications, **including those on mass transport of species**. Conversely, one could work directly with  $\mathbf{V}_i$  in Eq. (23) to whichever complexity is desired.

## Why is enthalpy conservation important?

There are combustion applications where the system's behavior is controlled by chemical kinetics, which are very sensitive to temperature, and lack of enthalpy conservation results in subtle changes in temperature and system behavior!

Furthermore, enthalpy conservation can (and should!) be checked when implementing or using a new numerical combustion code.

# The temperature transport eqn I

Temperature is not a conserved variable, yet, it is often solved for within the low Mach number form of reactive N-S equations.



Start with applying the chain rule to the definition of the material derivative of  $h$  for a mixture of ideal gases:

$$\rho \frac{Dh}{Dt} = \sum_{i=1}^K h_i(T) \rho \frac{DY_i}{Dt} + \rho C_p \frac{DT}{Dt}. \quad (27)$$

Now substitute Eq. (22) and Eq. (23) into Eq. (27) to obtain

$$\begin{aligned} \rho C_p \frac{DT}{dt} &= \frac{Dp}{Dt} + \nabla \cdot (\lambda \nabla T) - \nabla \cdot \left( \sum_i h_i(T) \rho Y_i \mathbf{v}_i \right) + \sum_i h_i(T) \nabla \cdot (\rho Y_i \mathbf{v}_i) + \dot{\omega}'_T \\ &= \frac{Dp}{Dt} + \nabla \cdot (\lambda \nabla T) + \dot{\omega}'_T + \sum_i C_{p,i} (-\rho Y_i \mathbf{v}_i) \cdot \nabla T \\ &= \frac{Dp}{Dt} + C_p \nabla \cdot (\rho \mathcal{D} \nabla T) + \rho \mathcal{D} \nabla T \cdot \nabla C_p + \dot{\omega}'_T + \sum_i C_{p,i} (-\rho Y_i \mathbf{v}_i) \cdot \nabla T \end{aligned} \quad (28)$$

# The temperature transport eqn II



- The first term  $Dp/Dt$  reflects the effect of pressure changes on enthalpy
- The second term  $(\nabla \cdot (\nabla T))$  is a classic diffusive term
- The third term  $(\nabla T \cdot \nabla C_p)$  is the second portion of the diffusive term and reflects spatial inhomogeneities in  $C_p$ . It is often neglected (or simply “forgotten” by mistake).
- The fourth term ( $\dot{\omega}'_T$ ) represents changes in temperature due to reactions

$$\dot{\omega}'_T = - \sum_{i=1}^K h_i(T) \dot{\omega}_i \quad (29)$$

- The fifth term  $(\mathbf{V}_i \cdot \nabla T)$  represents changes in temperature due to mass (i.e, enthalpy) transport. Depending on the closure model for  $\mathbf{V}_i$ , various forms of the temperature equation arise.

# The temperature transport eqn III



Assume Fick's law applies for the description of  $\mathbf{V}_i$

$$Y_i \mathbf{V}_i = -\mathcal{D} \nabla Y_i, \quad (30)$$

so that Eq. (28) becomes

$$\rho C_p \frac{DT}{Dt} = \frac{Dp}{Dt} + \nabla \cdot (\lambda \nabla T) + \dot{\omega}_T' + \sum_{i=1}^K \rho \mathcal{D} C_{p,i} \nabla T \cdot \nabla Y_i \quad (31)$$

If we assume that  $C_{p,i}(T) = C_p(T)$ , then the last term on the r.h.s. of Eq. (31) is zero due to  $\sum \nabla Y_i = 0$ , we obtain a very common form of the temperature equation:

$$\rho C_p \frac{DT}{Dt} = \frac{Dp}{Dt} + \nabla \cdot (\lambda \nabla T) + \dot{\omega}_T. \quad (32)$$

*NOTE. Eq. (32) is valid under several assumptions, including Fick's law and specific heat, which is the same for all species.*



# Software tools

# Two related challenges



There exist two major practical challenges in numerical combustion

- Firstly, one needs to manage the implementation of physical models for thermodynamic and transport properties, and kinetic mechanisms into working codes.
- A second related challenge is the archival, organization, and usage of the model parameters for the above physical models, e.g., rate parameters for kinetics, coefficients for thermodynamics data, etc.

*There exist available (open-source) libraries that one may leverage to effectively query physical models, i.e., calculate thermodynamic and transport properties, and evaluate chemical source terms.*

# The CHEMKIN legacy I



CHEMKIN is a software library developed in the 1980s at Sandia National Laboratories (Livermore) by Kee, Miller, and many others. See Technical report SAND-89-8009: "Chemkin-II: A Fortran Chemical Kinetics Package for the Analysis of Gas-Phase Chemical Kinetics".

*"Chemkin is a software package whose purpose is to facilitate the formation, solution, and interpretation of problems involving elementary gas-phase chemical kinetics. It provides an especially flexible and powerful tool for incorporating complex chemical kinetics into simulations of fluid dynamics. [...]"*

After the initial development of CHEMKIN as a library for computing thermodynamic, transport, and chemical kinetics, several well known applications were implemented: PREMIX (laminar premixed flames), OPPDIF (counterflow flames), SENKIN (zero-dimensional reactor), etc.

# Two of the people behind the remarkable success of CHEMKIN



**Robert J. Kee**  
*Colorado School of Mines  
Golden, Colorado, USA*



**James A. Miller**  
*Argonne National Lab,  
Argonne, Illinois, USA*

# The CHEMKIN legacy II



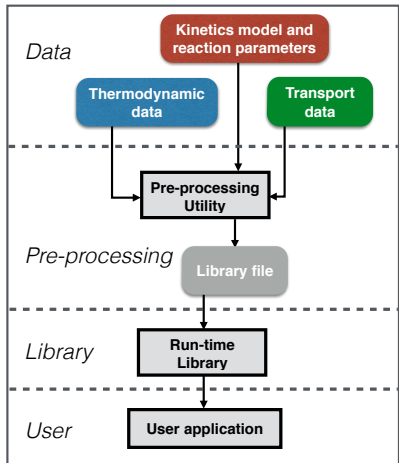
In the late 1990s, the CHEMKIN library was acquired by Reaction Design and turned into a commercial product (CHEMKIN-PRO). Reaction Design has been recently acquired by ANSYS.

The legacy of CHEMKIN is tremendous, with many groups still using the original CHEMKIN-II source or its commercial version (CHEMKIN-PRO).

In addition, many of the recently developed software libraries that enable numerical combustion borrow concepts, data structures, and input files from CHEMKIN.

An example of this legacy is the fact that the most used ASCII file format for combustion models is the “CHEMKIN format” (more later): *Combustion models are exchanged “using CHEMKIN files”*

# Example workflow and usage



- Assemble a set of data files which contain information about the kinetics model, thermodynamic and transport data (i.e., a **combustion model**)
- Run the files through a pre-processor utility, which is usually distributed with the software suite. This step produces a “library file”.
- Implement the appropriate interfaces in the source code of the user’s application and link the library
- At run time, calls to the library will return the desired quantities (e.g., reaction rates, mixture viscosity, etc.)

# Libraries and software suites I



- **CHEMKIN-II.** If the source was acquired prior to 1998, when CHEMKIN was turned over to a for-profit company (Reaction Design), then the user is entitled to use the code. **It is illegal to re-distribute.**
- **Cantera.** Conceived and developed by Prof. David Goodwin (Caltech), Cantera has now become a thriving open source project with significant community support.

It provides most of the CHEMKIN-PRO functionality in an open-source framework and is a very extensive collection of tools for kinetics, thermodynamics, transport, including computations of one-dimensional flames, equilibrium, etc.

It provides interfaces for FORTRAN, Python, C/C++, and Matlab, making it a very flexible platform.

More at <http://www.cantera.org>.

# Libraries and software suites II



- **FlameMaster.** A collection of utilities to compute one-dimensional premixed and nonpremixed flames. Developed and maintained by the Institute for Combustion Technology at RWTH Aachen (Dr. Heinz Pitsch).

It is written in C++ and provides its own set of thermodynamic, transport, and kinetics libraries, which are not easily accessible to the user.

More at

<http://www.itv.rwth-aachen.de/en/downloads/flamemaster/>.

- **OpenSmoke.** A collection of tools developed and maintained by Politecnico di Milano (Cuoci, A., Frassoldati, T. Faravelli, E. Ranzi) to solve laminar flames with detailed kinetics.

More at <http://www.opensmoke.polimi.it>.

# Libraries and software suites III



- **TChem.** The TChem toolkit is a software library that enables numerical simulations using complex chemistry. It is developed and maintained by Dr. Cosmin Safta at Sandia National Laboratories (Livermore).

The library contains several functions that provide analytically computed Jacobian matrices necessary for the efficient time advancement and analysis of detailed kinetic models.

More at <http://www.sandia.gov/tchem>



# Thermodynamics

# Basic definitions

The enthalpy of species  $k$  is such that:

$$h_k = \underbrace{\int_{T_0}^T C_{pk} dT}_{\text{sensible}} + \underbrace{\Delta h_{f,k}^o}_{\text{chemical}} \quad (33)$$

$T$  is the temperature and  $\Delta h_{f,k}^o$  is the mass enthalpy of formation of species  $k$  at the reference temperature  $T_0$ . The standard reference state used to tabulate formation enthalpies is usually set to  $T_0 = 298.15$  K.

The energy of species  $k$  is defined as:

$$e_k = e_{sk} + \Delta h_{f,k}^o \quad (34)$$

where  $e_{sk}$  is the sensible energy:

$$e_{sk} = \int_{T_0}^T C_{vk} dT - RT_0/W_k \quad C_{pk} - C_{vk} = R/W_k \quad (35)$$

$R = 8.314$  J/(mole K) is the perfect gas constant and  $W_k$  is the atomic weight of species  $k$ .



# $\Delta h_{f,k}^o$ for selected species



Species	$W_k$ (kg/mol)	$\Delta h_{f,k}^o$ (kJ/kg)	$\Delta h_{f,k}^{o,m}$ (kJ/mole)
$\text{CH}_4$	0.016	-4675	-74.8
$\text{C}_3\text{H}_8$	0.044	-2360	-103.8
$\text{C}_8\text{H}_{18}$	0.114	-1829	-208.5
$\text{CO}_2$	0.044	-8943	-393.5
$\text{H}_2\text{O}$	0.018	-13435	-241.8
$\text{O}_2$	0.032	0	0
$\text{H}_2$	0.002	0	0
$\text{N}_2$	0.028	0	0

Table: Molecular mass  $W_k$  (kg/mol) and formation enthalpies  $\Delta h_{f,k}^o$  (kJ/kg), and  $\Delta h_{f,k}^{o,m}$  (kJ/mole) at  $T_0 = 298.15$  K.

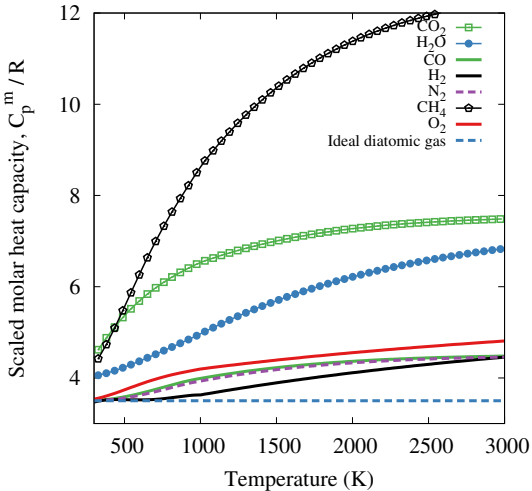
# Scaled molar heat capacities



Heat capacities at constant pressure vary with temperature and across species.

*How significant are those dependencies?*

The scaled molar heat capacities at constant pressure ( $C_p^m/R$ ) of  $\text{CO}_2$ ,  $\text{CO}$ ,  $\text{H}_2\text{O}$ ,  $\text{H}_2$ ,  $\text{N}_2$ ,  $\text{CH}_4$ , and  $\text{O}_2$  are shown in the plot on the right.



# Databases for thermodynamics data



Thermodynamic databases are a key component of efforts in numerical combustion. Three typical sources:

- Thermodynamics data are obtained as part of a “combustion model” comprising thermodynamics, transport, and kinetic models (e.g., the GRIMech 3.0 methane mechanism)
- NASA Glenn Coefficients for Calculating Thermodynamic Properties of Individual Species (NASA/TP2002-211556) Available at <http://www.grc.nasa.gov/WWW/CEAWeb/>.
- Prof. Burcat’s Data base: Ideal Gas Thermodynamic Data in Polynomial Form for Combustion and Air Pollution Use. Available at <http://garfield.chem.elte.hu/Burcat/burcat.html> or <http://burcat.technion.ac.il/dir/>.

*Note that the report TP2002-211556 has a great introduction to the formats of thermodynamics data used in combustion codes, i.e., the so-called “NASA polynomials”, as well as an in-depth discussion of standard and reference states*

# NASA polynomials



First use a fourth-order polynomial<sup>3</sup>to fit  $C_p/R$  for a species:

$$\frac{C_{pk}}{R} = a_1 + a_2 T + a_3 T^2 + a_4 T^3 + a_5 T^4 \quad (36)$$

Then integrate  $C_{p,k}/R$  and  $C_{p,k}/RT$  from  $T_0$  to  $T$  to obtain  $H/RT$  and  $S/R$

$$\frac{H_k}{RT} = a_1 + \frac{a_2}{2} T + \frac{a_3}{3} T^2 + \frac{a_4}{4} T^3 + \frac{a_5}{5} T^4 + \frac{a_6}{T} \quad (37)$$

$$\frac{S_k}{R} = a_1 \ln T + a_2 T + \frac{a_3}{2} T^2 + \frac{a_4}{3} T^3 + \frac{a_5}{4} T^4 + a_7 \quad (38)$$

Typically, “standard conditions” means  $p = 1$  atm and  $T_0 = 273.15$  K.

---

<sup>3</sup>One needs to exercise extra care when assembling thermodynamics coefficients from more than one source or novel sources. E.g., in the 2002 report NASA/TP2002-211556, a 7 coefficient fit is adopted:  $C_p(T)/R = a_1 T^{-2} + a_2 T^{-1} + a_3 + a_4 T + a_5 T^2 + a_6 T^3 + a_7 T^4$ , where the coefficients **are not the same** as in the fourth-order polynomial used in the original NASA polynomials (e.g., McBride et al., 1994).

# Thermodynamics



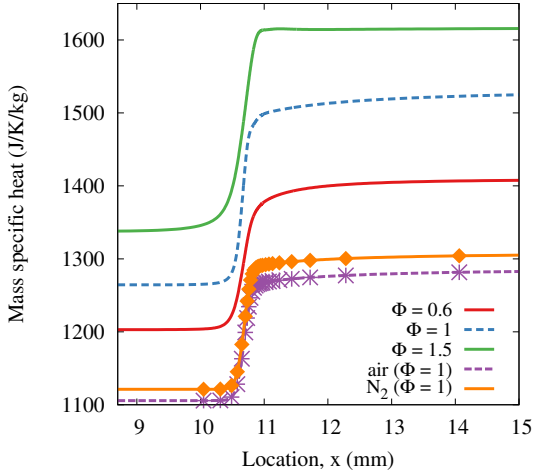
Below the CO<sub>2</sub> entry from Burcat's database.

CO2	L	7/88C	10	2	0	0G	200.000	6000.000	1000.	1
0.46365111E+01	0.27414569E-02	-0.99589759E-06	0.16038666E-09	-0.91619857E-14						2
-0.49024904E+05	-0.19348955E+01	0.23568130E+01	0.89841299E-02	-0.71220632E-05						3
0.24573008E-08	-0.14288548E-12	-0.48371971E+05	0.99009035E+01	-0.47328105E+05						4

- This is the “original” NASA format by McBride et al., also used by CHEMKIN
- Note that the entry above features 4 lines of 80 characters each
- The first line is a header indicating the species name, elemental composition, and the range of temperatures for the fits
- The second, third, and fourth lines contain  $7 \times 2 + 1 = 14 + 1 = 15$  coefficients for the polynomials

*Note the 15-th entry, which is ignored by most programs in use in the combustion community. It's actually H(298.15)/R.*

# Mass specific heat across flames



For the most part, combustion occurs in air, which is 79%  $N_2$  by volume.

Since  $C_p = \sum_{i=1}^M C_{p,i} y_i$ , the specific heat at constant pressure is mostly this of  $N_2$ .

On the left, the variation of  $C_p$  across a premixed  $CH_4$ /air flame at 1 atm (800 K unburnt gases).

In the case  $\Phi = 0.6$ ,  $C_p$  increases by  $\approx 17\%$  ( $C_{p,u} = 1202 \text{ kJ/kg-K}$  to  $C_{p,b} = 1409 \text{ kJ/kg-K}$ ) across the flame due to temperature changes.



# Transport

# Introduction



In general, all transport properties should be treated as functions of the thermo-chemical state of the mixture:  $T$ ,  $p$ , and  $\mathbf{Y}$ .

- $\mu$ : dynamic viscosity of the mixture (Pa-s)
- $\lambda$ : thermal conductivity of the mixture (W/m-K)
- $\mathcal{D}_{ij}$ : binary diffusion coefficients for species components ( $\text{m}^2/\text{s}$ )

Widely adopted models for transport properties are based on the Chapman-Enskog theory for a multicomponent gas mixtures under thermal and chemical equilibrium (Chapman and Cowling, 1991).

*The theory is centered around the concept of binary interactions between colliding molecules. Collisions are described well by potential functions (e.g., Lennard-Jones and Stockmayer potentials) in the regime of interest for most combustion applications.*

# Molecular transport properties



Sample “tran.dat” data file from GRIMech 3.0.

Species ID		$\epsilon/k_B$	$\sigma$	$\mu$	$\alpha$	$Z_{rot}$
AR	0	136.500	3.330	0.000	0.000	0.000
CH4	2	141.400	3.746	0.000	2.600	13.000
CO	1	98.100	3.650	0.000	1.950	1.800
CO2	1	244.000	3.763	0.000	2.650	2.100
H2O	2	572.400	2.605	1.844	0.000	4.000
N2	1	97.530	3.621	0.000	1.760	4.000
O	0	80.000	2.750	0.000	0.000	0.000
O2	1	107.400	3.458	0.000	1.600	3.800
OH	1	80.000	2.750	0.000	0.000	0.000

Configuration index  
Potential well-depth (K)  
Collision diameter ( $\text{\AA}$ )  
Dipole moment (Debye)  
Polarizability ( $\text{\AA}^3$ )  
Rotational relaxation collision number at 298 K

Note that the parameters that describe the binary interactions between pairs of molecules are obtained from the parameters of individual species.

# Formulas for viscosity I



The dynamic viscosity  $\mu$  in a gas mixture is defined as (Bird et al., 2007):

$$\mu = \sum_{i=1}^K \frac{X_k \mu_k}{\sum_{j=1}^K X_j \Phi_{kj}} \quad (39)$$

where  $\mu_k$  is the viscosity for the pure species,  $X_k$  is the species mole fraction in the mixture, and  $\Phi_{kj}$  is defined as:

$$\Phi_{kj} = \frac{1}{\sqrt{8}} \left( 1 + \frac{W_k}{W_j} \right)^{-\frac{1}{2}} \left( 1 + \left( \frac{\mu_k}{\mu_j} \right)^{\frac{1}{2}} \left( \frac{W_j}{W_k} \right)^{\frac{1}{4}} \right)^2 \quad (40)$$

*Note that the evaluation of viscosity requires a double-loop over all species. For mechanisms featuring a large number of species, the computational cost becomes prohibitive rather rapidly.*

# Formulas for viscosity II



The viscosity for a pure species is computed as (Bird et al., 2007):

$$\mu_k = \frac{5}{16} \frac{\sqrt{\pi m_k k_B T}}{\pi \sigma_k^2 \Omega^{(2,2)}} = \frac{5}{16} \frac{\sqrt{\pi m_k k_B}}{\pi \sigma_k^2} \left( \frac{T}{\Omega^{(2,2)}} \right) \quad (41)$$

where  $\Omega^{(2,2)}$  is the collision integral, which depends on the “reduced temperature”  $T^* = k_B T / \epsilon_k$  and the “reduced dipole moment”  $\delta = \eta_k / 2\epsilon_k \sigma_k^3$ .

In the definitions of  $T^*$  and  $\delta$ ,  $\sigma_k$ ,  $\epsilon_k$ , and  $\eta_k$  are the Lennard-Jones collision diameter, potential well depth, and dipole moment for the species, which are typically read in from a database.

*Obviously,  $\mu$  is a function of the mixture composition  $\mathbf{x}$  and temperature  $T$ , and thus it cannot be pre-computed in advance.*



# Table of $\Omega^{(2,2)}$

TABLE V.  $\langle \Omega^{(2,2)*} \rangle$ .

$T^{\frac{\delta}{\alpha}}$	0	0.25	0.50	0.75	1.0	1.5	2.0	2.5
0.1	4.1005	4.266	4.833	5.742	6.729	8.624	10.34	11.89
0.2	3.2626	3.305	3.516	3.914	4.433	5.570	6.637	7.618
0.3	2.8399	2.836	2.936	3.168	3.511	4.329	5.126	5.874
0.4	2.5310	2.522	2.586	2.749	3.004	3.640	4.282	4.895
0.5	2.2837	2.277	2.329	2.460	2.665	3.187	3.727	4.249
0.6	2.0838	2.081	2.130	2.243	2.417	2.862	3.329	3.786
0.7	1.9220	1.924	1.970	2.072	2.225	2.614	3.028	3.435
0.8	1.7902	1.795	1.840	1.934	2.070	2.417	2.788	3.156
0.9	1.6823	1.689	1.733	1.820	1.944	2.258	2.596	2.933
1.0	1.5929	1.601	1.644	1.725	1.838	2.124	2.435	2.746
1.2	1.4551	1.465	1.504	1.574	1.670	1.913	2.181	2.451
1.4	1.3551	1.365	1.400	1.461	1.544	1.754	1.989	2.228
1.6	1.2800	1.289	1.321	1.374	1.447	1.630	1.838	2.053
1.8	1.2219	1.231	1.259	1.306	1.370	1.532	1.718	1.912
2.0	1.1757	1.184	1.209	1.251	1.307	1.451	1.618	1.795
2.5	1.0933	1.100	1.119	1.150	1.193	1.304	1.435	1.578
3.0	1.0388	1.044	1.059	1.083	1.117	1.204	1.310	1.428
3.5	0.99963	1.004	1.016	1.035	1.062	1.133	1.220	1.319
4.0	0.96998	0.9732	0.9830	0.9991	1.021	1.079	1.153	1.236
5.0	0.92676	0.9291	0.9360	0.9473	0.9628	1.005	1.058	1.121
6.0	0.89616	0.8979	0.9030	0.9114	0.9230	0.9545	0.9955	1.044
7.0	0.87272	0.8741	0.8780	0.8845	0.8935	0.9181	0.9505	0.9893
8.0	0.85379	0.8549	0.8580	0.8632	0.8703	0.8901	0.9164	0.9482
9.0	0.83795	0.8388	0.8414	0.8456	0.8515	0.8678	0.8895	0.9160
10.0	0.82435	0.8251	0.8273	0.8308	0.8356	0.8493	0.8676	0.8901
12.0	0.80184	0.8024	0.8039	0.8065	0.8101	0.8201	0.8337	0.8504
14.0	0.78363	0.7840	0.7852	0.7872	0.7899	0.7976	0.8081	0.8212
16.0	0.76834	0.7687	0.7696	0.7712	0.7733	0.7794	0.7878	0.7983
18.0	0.75518	0.7554	0.7562	0.7575	0.7592	0.7642	0.7711	0.7797
20.0	0.74364	0.7438	0.7445	0.7455	0.7470	0.7512	0.7569	0.7642
25.0	0.71982	0.7200	0.7204	0.7211	0.7221	0.7250	0.7289	0.7339
30.0	0.70097	0.7011	0.7014	0.7019	0.7026	0.7047	0.7076	0.7112
35.0	0.68545	0.6855	0.6858	0.6861	0.6867	0.6883	0.6905	0.6932
40.0	0.67232	0.6724	0.6726	0.6728	0.6733	0.6745	0.6762	0.6784
50.0	0.65099	0.6510	0.6512	0.6513	0.6516	0.6524	0.6534	0.6546
75.0	0.61397	0.6141	0.6143	0.6145	0.6147	0.6148	0.6148	0.6147
100.0	0.58870	0.5889	0.5894	0.5900	0.5903	0.5901	0.5895	0.5885

# Algorithm of viscosity computation



## Pre-processing step.

- Read thermal and transport properties of species
- Pre-compute all species properties
- Based on these properties and the table of  $\Omega^{(2,2)}$ , generate polynomial coefficients for  $\Omega^{(2,2)}(T)$

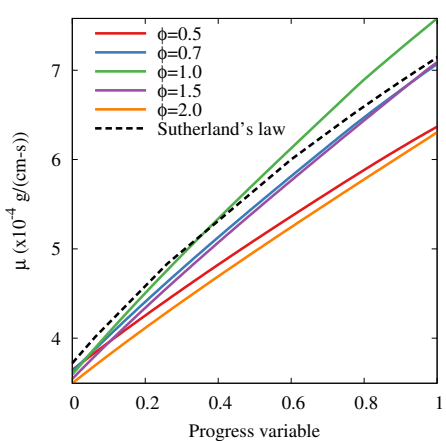
## At run time.

- Obtain temperature and mole fractions of all species
- Compute reduced temperature and dipole moment
- Use the polynomial coefficients and temperature to compute  $\Omega^{(2,2)}$
- Compute the viscosities for each single species by Eq. (41)
- Compute the mixture viscosity of the mixture with Eqs. (39) and (40)

# Dynamic viscosity



Let us consider a CH<sub>4</sub>/air flame with  $T_u = 800$  K at 1 atm



Sutherland's formula

$$\mu = \mu_0 \frac{T_0 + C}{T + C} \left( \frac{T}{T_0} \right)^{3/2} \quad (42)$$

where  $C = 120$  K,  $T_0 = 291.15$  K, and  $\mu_0 = 18.27 \mu\text{Pa}\cdot\text{s}$  for air.

$\mu$  does not depend on pressure, as implied by the kinetic theory of gases (Vincenti and Krüger, 1965):  $\mu = \beta \rho \ell \langle C \rangle$ , where  $\beta$  is a constant,  $\rho$  is density,  $\langle C \rangle$  is the average molecular speed ( $\propto T^{1/2}$ ) and  $\ell$  is the mean free path ( $\rho \ell \approx \text{const}$ ).

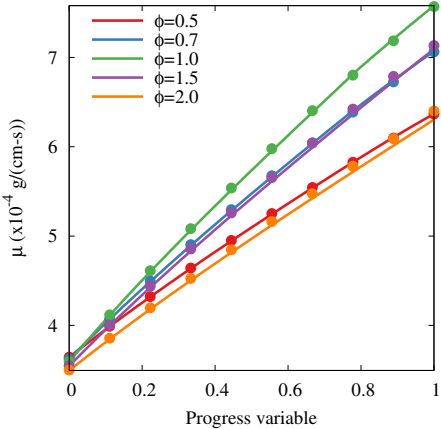
# Reduced vs. full viscosity



If there are a large number of species, computing  $\mu$  is prohibitively expensive, but one can model the mixture with a reduced set of major species.

*But how effective (and accurate) is the “reduced viscosity”?*

The figure on the right shows the variation of  $\mu$  across several 1 atm CH<sub>4</sub>/air flames at various equivalence ratios.



The lines are the “detailed viscosity” (including all 53 species in GRIMech 3.0), while the symbols are the “reduced viscosity” based on CH<sub>4</sub>, N<sub>2</sub>, O<sub>2</sub>, H<sub>2</sub>O, CO, and CO<sub>2</sub>.

# Thermal diffusion coefficient

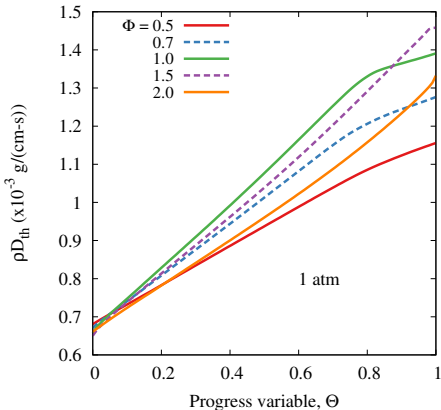


The thermal diffusion coefficient

$D_{th} = \lambda / \rho C_p$  ( $\text{m}^2/\text{s}$ ) is key to diffusive transport processes (enthalpy, temperature, and species):

$$D_{th} = \frac{\lambda}{\rho C_p}$$

where  $\lambda$  ( $\text{W}/(\text{m}\cdot\text{K})$ ) is the thermal conductivity,  $\rho$  is density, and  $C_p$  is the specific heat at constant pressure for the mixture.



*A rather common assumption is to let  $\rho D_{th} = \text{const}$  for simplicity (see theoretical treatment of laminar flame speeds). In reality, there is a dependence on temperature, as shown in the figure above.*

# Lewis numbers



Recall that a significant simplification to the closure for the diffusive velocity for species is the “constant Lewis number” model (Poinsot and Veynante, 2005):

$$\rho Y_i \mathbf{v}_i = -\rho \mathcal{D}_i \frac{Y_i}{X_i} \nabla X_i = -\frac{\rho \mathcal{D}}{\text{Le}_i} Y_i \frac{\nabla W}{W} - \frac{\rho \mathcal{D}}{\text{Le}_i} \nabla Y_i. \quad (43)$$

where we let:

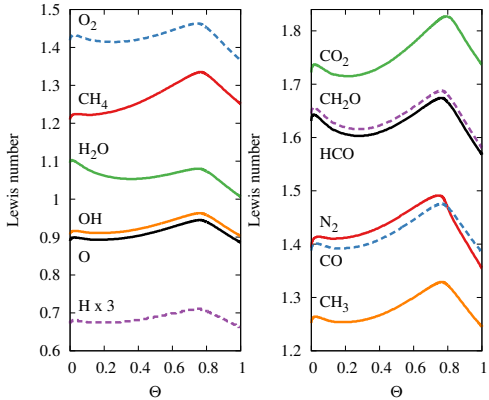
$$\text{Le}_i = \frac{\mathcal{D}}{\mathcal{D}_i}. \quad (44)$$

*But just how constant are the Lewis numbers of individual species?*

# Lewis numbers



Let us consider the variation of Lewis numbers across a premixed  $\text{CH}_4/\text{air}$  flame at  $T_u = 800 \text{ K}$  and  $1 \text{ atm}$



Species	0.5	1.0	1.5
$\text{H}_2\text{O}$	1.039	1.055	1.097
$\text{CH}_4$	1.240	1.260	1.303
$\text{N}_2$	1.326	1.436	1.559
$\text{CO}$	1.382	1.414	1.470
$\text{O}_2$	1.396	1.424	1.475
$\text{CO}_2$	1.706	1.737	1.801
H	0.220	0.228	0.241
O	0.885	0.906	0.944
OH	0.902	0.924	0.962
$\text{CH}_3$	1.241	1.271	1.325
HCO	1.585	1.614	1.676
$\text{CH}_2\text{O}$	1.598	1.626	1.689

Shown on the left are the Lewis numbers of various species for a stoichiometric methane/air flame  $\Phi = 1$ .

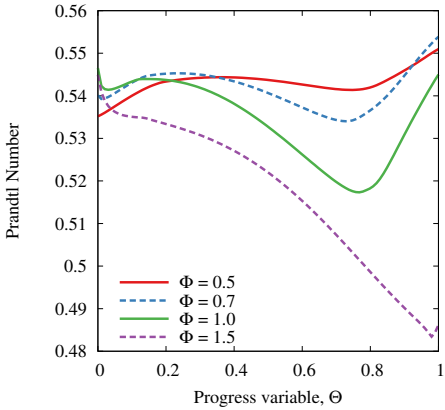
# Prandtl number



The Prandtl number is defined as  $\text{Pr} = \nu/\mathcal{D}$  and is approximately constant but not equal to the Prandtl's number of air ( $\text{Pr} \approx 0.71$  at  $20^\circ\text{C}$ ).

As shown on the right, the Prandtl number for methane flames at  $T_u = 800$  K varies between 0.48 and 0.55 across the flame and depending on  $\Phi$ . Let:

$$\text{Pr} \approx 0.54$$



*Recall that the Prandtl number does not depend on pressure.*



# Kinetics

# Chemical Kinetics



Consider a chemical system of  $N$  species reacting through  $R$  reactions:

$$\boxed{\sum_{k=1}^N \nu'_{kj} \mu_k \rightleftharpoons \sum_{k=1}^N \nu''_{kj} \mu_k \quad \text{for } j = 1, \dots, R} \quad (45)$$

where  $\mu_k$  is a symbol for species  $k$ ,  $\nu'_{kj}$  and  $\nu''_{kj}$  are the molar stoichiometric coefficients of species  $k$  in reaction  $j$ .

Mass conservation enforces:

$$\sum_{k=1}^N \nu'_{kj} W_k = \sum_{k=1}^N \nu''_{kj} W_k \quad \text{or} \quad \sum_{k=1}^N \nu_{kj} W_k = 0 \quad \text{for } j = 1, \dots, R \quad (46)$$

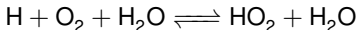
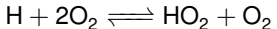
$$\nu_{kj} = \nu''_{kj} - \nu'_{kj} \quad (47)$$

*Any robust chemical kinetics library will check “stoichiometric consistency”, i.e., mass conservation, for each input reaction*

# An example of a mechanism



Consider the following reactions which involve the species H, O<sub>2</sub>, HO<sub>2</sub>, H<sub>2</sub>O, O, and OH



For this example, let  $\mu_1 = H$ ,  $\mu_2 = O_2$ ,  $\mu_3 = HO_2$ ,  $\mu_4 = H_2O$ ,  $\mu_5 = O$ ,  $\mu_6 = OH$ .

$$\nu'_{11} = 1, \nu'_{21} = 2, \nu'_{3,1} = 0, \nu'_{41} = 0, \nu'_{51} = 0, \nu'_{61} = 0.$$

$$\nu'_{12} = 1, \nu'_{22} = 1, \nu'_{3,2} = 0, \nu'_{41} = 1, \nu'_{52} = 0, \nu'_{62} = 0.$$

$$\nu'_{13} = 1, \nu'_{23} = 1, \nu'_{3,3} = 0, \nu'_{41} = 0, \nu'_{53} = 0, \nu'_{63} = 0.$$

$$\nu''_{11} = 0, \nu''_{21} = 0, \nu''_{3,1} = 1, \nu''_{41} = 0, \nu''_{51} = 0, \nu''_{61} = 0.$$

$$\nu''_{12} = 0, \nu''_{22} = 0, \nu''_{3,2} = 1, \nu''_{41} = 1, \nu''_{52} = 0, \nu''_{62} = 0.$$

$$\nu''_{13} = 0, \nu''_{23} = 0, \nu''_{3,3} = 0, \nu''_{41} = 0, \nu''_{53} = 1, \nu''_{63} = 1.$$

# Chemical Kinetics



For simplicity, only mass based rates are used. For species  $k$ , the rate  $\dot{\Omega}_k$  is the sum of rates  $\dot{\Omega}_{kj}$  ( $\text{g}/\text{cm}^3\cdot\text{s}$ ) produced by all  $R$  reactions

$$\dot{\Omega}_k = \sum_{j=1}^R \dot{\Omega}_{kj} = W_k \sum_{j=1}^R \nu_{kj} Q_j \quad \text{with} \quad \frac{\dot{\Omega}_{kj}}{W_k \nu_{kj}} = Q_j, \quad (48)$$

where  $Q_j$  ( $\text{mol}/\text{cm}^3\cdot\text{s}$ ) is the “rate of progress” of reaction  $j$ .

Summing all reactions rates  $\dot{\Omega}_j$  and using Eq. 46, one obtains:

$$\sum_{k=1}^N \dot{\Omega}_k = \sum_{j=1}^R \left( Q_j \sum_{k=1}^N W_k \nu_{kj} \right) \xrightarrow{0} 0, \quad (49)$$

which illustrates that the total mass is conserved.

# Chemical Kinetics



The “rate of progress”  $\mathcal{Q}_j$  of reaction  $j$  is written:

$$\mathcal{Q}_j = k_j^f \prod_{k=1}^N c_k^{\nu'_{kj}} - k_j^r \prod_{k=1}^N c_k^{\nu''_{kj}} \quad (50)$$

where  $k_j^f$  and  $k_j^r$  are the “forward and reverse rate constants” for reaction  $j$ . The two rates are linked through the equilibrium constant of the reaction (see details later).

Note, that the rate of progress is proportional to the product of molar concentrations  $c_k = \rho Y_k / W_k$ .

*A reaction’s “rate constants” are not really constants, as they are function of temperature!*

# Chemical kinetics



The rates constant are usually modeled using the **empirical** Arrhenius law:

$$k_j^f = A_j T^{n_j} \exp\left(-\frac{E_j}{RT}\right) = A_j T^{n_j} \exp\left(-\frac{T_j^a}{T}\right) \quad (51)$$

where  $A$  is the pre-exponential factor,  $n$  is the temperature exponent, and  $E$  is the activation energy ( $T^a = E/R$  is the activation temperature).

- The Arrhenius law is an empirical fit to observed rate constants and there may be reactions that do not confirm to the Arrhenius format
- CGS is the most commonly employed system of units for rate parameters.
- The actual units of  $k^f$  and  $k^r$  (and thus of the group  $AT^n$ ) depend on the number of reactant and product species and vary reaction by reaction
- The best one can do is to say that units are cm, mol, s, K, and cal

# Equilibrium constant



Let  $K_j(T)$  indicate the equilibrium constant for reaction  $j$

$$K_j(T) = \exp \left[ -\frac{1}{RT} \sum_{k=1}^N \nu_{kj} g_k(T, p_0) \right] = \prod_{k=1}^N \left( \frac{x_k p}{p_0} \right)^{\nu_{kj}} \quad (52)$$

for a reaction  $\sum \nu_{kj} \mu_k = 0$ .

In Eq. (52),  $g_k = g_k(T, p_0) = h_k(T) - Ts_k(T, p_0)$  is the Gibbs free energy per unit mole of species  $k$ ,  $x_k$  is the mole fraction, and  $p$  is the mixture pressure.

Note that the equilibrium constant is **solely a function of temperature** and it is computed at a “reference pressure”  $p_0$ , usually set to 1 atm.

*How can one use  $K(T)$  to link the forward and backward rate constants?*

# Usage in chemical kinetics



One may rewrite Eq. (52) as follows

$$K_j(T) = \left(10^6 \times \frac{\mathcal{R}T}{p_0}\right)^{\sum \nu_{kj}} \prod c_k^{\nu_{kj}} = \left(10^6 \times \frac{\mathcal{R}T}{p_0}\right)^{\sum \nu_{kj}} \frac{k_j^f}{k_j^r}, \quad (53)$$

where  $\mathcal{R} = 8.314 \text{ J/mol-K}$  is the universal gas constant,  $p_0$  (Pa) is the reference pressure at which  $g_k(T, p_0)$  is calculated, and  $c_k$  is the concentration ( $\text{mol/cm}^3$ ) of species  $i$ .

Often times, one introduces  $K_j^c(T)$  defined as follows

$$K_j^c(T) = \frac{k_j^f}{k_j^r} = K_j(T) \left(10^{-6} \times \frac{p_0}{\mathcal{R}T}\right)^{\sum \nu_{kj}} \quad (54)$$

*The fact that the reverse rate constant of a reaction is computed from the equilibrium constant implies that chemical kinetics rates are affected by thermodynamic properties of the species.*

# Reaction Rate Constant

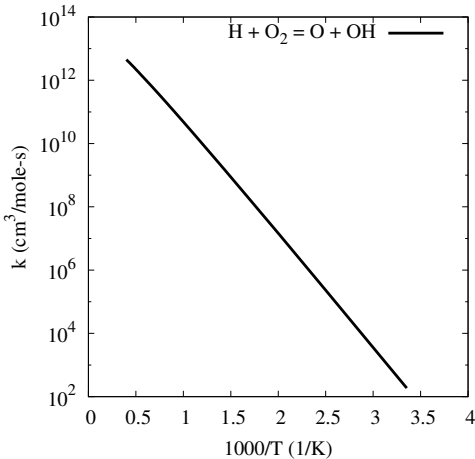


Consider the forward rate constant for the reaction

$$\text{H} + \text{O}_2 \rightleftharpoons \text{OH} + \text{O}$$

$$k = AT^n \exp(-E/RT) \quad (55)$$

where  $k$  ( $\text{cm}^3/\text{mol}\cdot\text{s}$ ) is the rate constant,  $A = 2.65\text{E+16}$ ,  $n = -0.6707$ , and  $E = 17.04$  kcal/mol.



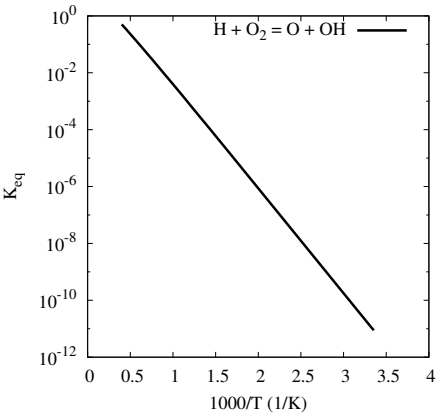
*When plotted as  $\log_{10} k$  versus  $1000/T$ , it is clear that the rate constant appears as a straight line. The temperature exponent results in a slight curvature.*

# Equilibrium Constant



Consider the equilibrium constant for the reaction  $\text{H} + \text{O}_2 \rightleftharpoons \text{OH} + \text{O}$

- $K^c = k^f / k^r < 1$  for  $T \leq 2500$  K indicates that  $k^r > k^f$  i.e., recombination of the two radicals OH and O is favored thermodynamically.
- Since  $\sum \nu_k = 0$ , i.e., the number of moles of products and reactants are the same, it is clear that  $K_j(T) = K_j^c(T)$ .
- The fact that  $\log_{10} K^c$  versus  $1000/T$  is a straight line, indicates that  $\sum_{k=1}^N \nu_{kj} g_k(T, p_0)$  is a weak function of temperature.



# The CHEMKIN format for kinetics inputs



Reaction parameters for hundreds of reactions are organized in “chemical kinetics mechanisms”, which are encoded in ASCII files according to a specific format.

For historical reasons, the most widely adopted format is the so called “CHEMKIN format”, which we shall discuss briefly here.

*The “CHEMKIN format” is by no means the best possible format, and other manners of storing reaction rate parameters exist, e.g., the “Cantera format”, which leverages the markup language XML.*

# Sample mechanism (CHEMKIN)

Sample of the GRI Mech 3.0<sup>10</sup> mechanism



Elements							
ELEMENTS	O	H	C	N	AR	Species	
END							
SPECIES							
H2	H	O	O2	OH	H2O	HO2	H2O2
C	CH	CH2	CH2(S)	CH3	CH4	CO	CO2
HCO	CH2O	CH2OH	CH3O	CH3OH	C2H	C2H2	C2H3
C2H4	C2H5	C2H6	HCCO	CH2CO	HCCOH	N	NH
NH2	NH3	NNH	NO	NO2	N2O	HNO	CN
HCN	H2CN	HCNN	HCNO	HOCN	HNCO	NCO	N2
AR	C3H7	C3H8	CH2CHO	CH3CHO			
END							
REACTIONS							
20+M=>O2+M					1.200E+17	-1.000	.00
H2/ 2.40/ H2O/15.40/ CH4/ 2.00/ CO/ 1.75/ CO2/ 3.60/ C2H6/ 3.00/ AR/ .83/							
O+H+M=>OH+M					5.000E+17	-1.000	.00
H2/2.00/ H2O/6.00/ CH4/2.00/ CO/1.50/ CO2/2.00/ C2H6/3.00/ AR/ .70/							
O+H2=>H+OH					3.870E+04	2.700	6260.00
O+HO2=>OH+O2					2.000E+13	.000	.00
O+H2O2=>OH+HO2					9.630E+06	2.000	4000.00
H+O2=>O+OH					2.650E+16	-.6707	17041.00
O+CH=>H+CO					5.700E+13	.000	.00
O+CH2=>H+HCO					8.000E+13	.000	.00

Reactions

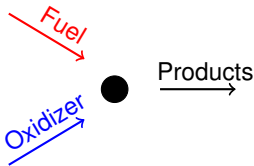
$A \uparrow$        $n \uparrow$        $E \uparrow$

<sup>10</sup>GRI-Mech is an optimized detailed chemical reaction mechanism for natural gas flames and ignition (see <http://combustion.berkeley.edu/gri-mech/>).

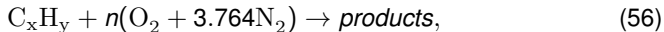


# Stoichiometry

# Stoichiometry: basic definitions



Consider air as an oxidizer and write down the stoichiometric reaction for air with one hydrocarbon molecule  $C_xH_y$ :

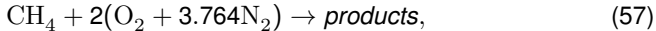


where  $n = x + y/4$  for a stoichiometric mixture.

For example, if the fuel is methane,  $CH_4$ , one has  $x = 1$ ,  $y = 4$ , and  $n = 2$ ; if the fuel is ethylene,  $C_2H_4$  and  $x = 2$ ,  $y = 4$ , and  $n = 3$ .

# Equivalence ratio $\Phi$

Once the stoichiometric formula is written



the next step is to write down the ratio of the mass fraction of oxidizer to the mass fraction of fuel for a stoichiometric mixture

$$\left. \frac{Y_O}{Y_F} \right|_{st} = \frac{n(W_{O_2} + 3.764W_{N_2})}{W_{fuel}} \quad (58)$$

For  $n = 2$ ,  $W_{O_2} = 32$ ,  $W_{N_2} = 28$ , and  $W_{\text{CH}_4} = 16$ :

$$\left. \frac{Y_O}{Y_F} \right|_{st} = 17.174 = s. \quad (59)$$

The above may be related to equivalence ratio  $\Phi$  and to mixture fraction  $Z$

$$\Phi = \frac{(Y_F/Y_O)}{(Y_F/Y_O)_{st}} \quad (60)$$

$$\frac{Y_F}{Y_O} = \left. \frac{Y_F}{Y_O} \right|_{st} \Phi = \frac{\Phi}{s} \quad (61)$$



# Mixture fraction $Z$



$$Z = \frac{Y_F}{Y_O + Y_F} = \frac{Y_F/Y_O}{1 + Y_F/Y_O} = \frac{\Phi}{\Phi + s} \quad (62)$$

For a stoichiometric mixture,  $\Phi = 1$  to give

$$Z_{st} = \frac{1}{1 + s} \quad (63)$$

For CH<sub>4</sub>,  $s = 17.174$  and  $Z_{st}$  becomes:

$$Z_{st} = 0.055 \quad (64)$$

Similarly for C<sub>2</sub>H<sub>4</sub>,  $n = 3$ ,  $W_{O_2} = 32$ ,  $W_{N_2} = 28$ , and  $W_{C_2H_4} = 28$ :

$$\left. \frac{Y_O}{Y_F} \right|_{st} = 14.7206 = s \quad (65)$$

For C<sub>2</sub>H<sub>4</sub>,  $s = 14.7206$ ,  $Z_{st}$  becomes:

$$Z_{st} = 0.0636 \quad (66)$$



# Laminar premixed flames

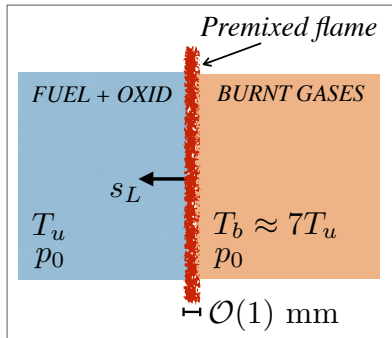
# Introduction



We shall consider the case of a one-dimensional (1D) laminar flame propagating into a premixed mixture of fuel and oxidizer (e.g., air and methane).

## Important 1D simplifications

- Absence of mixture and velocity gradients ahead of the flame
- Absence of aerodynamic stretch and curvature
- Steady propagation



*Even though there are simplifications, the main features of a premixed flames are retained: (a) a thin interface propagating at  $\mathcal{O}(1) \text{ m/s}$ ; (b) induces increase of temperature by  $T_b/T_u \approx 7$ ; (c) pressure remains constant  $p_b \approx p_u = p_0$ .*

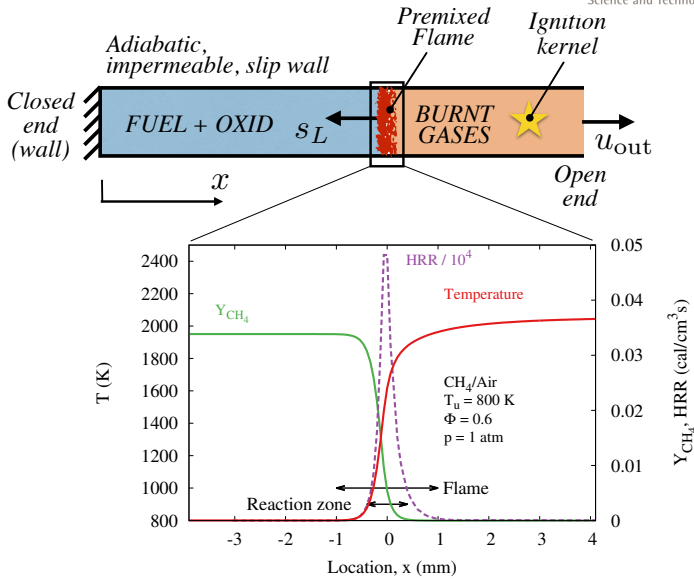
# Why focus on 1D laminar flames?



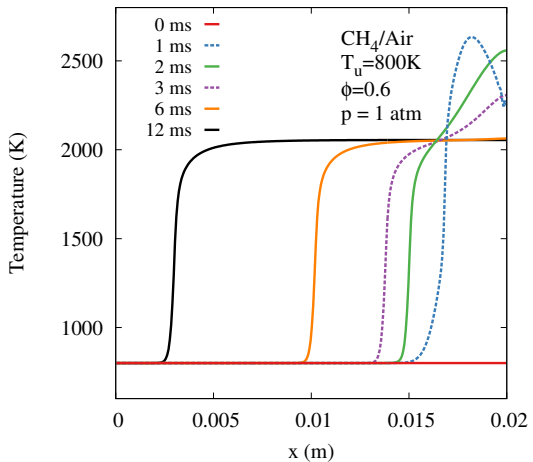
- It is one of the “canonical” problems in combustion, which allows for a comparison between theory, experiment, and computations
- The 1D nature implies that the flame is “unstretched”, providing a reference condition to build databases of laminar flame speeds for various fuels (Egolfopoulos et al., 2014)
- May be used to assess the “quality” of combustion models (thermodynamics, kinetics, and transport models)
- Laminar flames are viewed in many turbulent combustion models as “building blocks” for turbulent combustion closures

*Here we shall focus on the numerical solution of 1D laminar flames with complex chemical kinetics, thermodynamics, and transport models*

# A flame tube experiment



# Solving for a flame in a tube



- A tube is filled with a quiescent mixture of methane and air at  $T_u = 800 \text{ K}$  and  $1 \text{ atm}$
- A source of energy is placed towards the open end causing the temperature to increase locally (ignition kernel)
- A flame develops and after a few ms, a premixed flame is established

The flame propagates steadily right to left into the unburnt gases at a constant speed  $s_L \approx 125 \text{ cm/s}$

# Conservation equations I



The conservation equations are the reactive Navier-Stokes equations where the  $x$  components and derivatives are retained.

$$\frac{\partial \rho}{\partial t} + \frac{\partial \rho u}{\partial x} = 0 \quad (67)$$

$$\frac{\partial \rho Y_k}{\partial t} + \frac{\partial}{\partial x} (\rho(u + V_k)Y_k) = \dot{\omega}_k, \quad k = 1, N - 1 \quad (68)$$

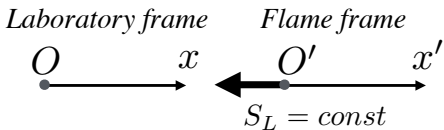
$$\rho C_p \left( \frac{\partial T}{\partial t} + u \frac{\partial T}{\partial x} \right) = \dot{\omega}_T + \frac{\partial}{\partial x} \left( \lambda \frac{\partial T}{\partial x} \right) + \rho \frac{\partial T}{\partial x} \left( \sum_{k=1}^N C_{p,k} Y_k V_k \right) \quad (69)$$

For reasons that will be clear shortly, there is no need to include the momentum equation to solve for the flame structure and the momentum equation serves the purpose of computing the dynamic pressure only.

# Conservation equations II



When the flame has settled, it propagates into quiescent, unburnt gases at a constant speed  $s_L$ , so that it is more advantageous to consider conservation equations written in an inertial frame of reference attached to the flame front



Recall that the Navier-Stokes equations are Galilean invariant, i.e., “the laws of motion are the same in all inertial frames”.

Of course, Galilean invariance with respect to a transformation of the reactive Navier-Stokes from the laboratory coordinate system to the flame's assumes that the flame is moving at **constant** speed, i.e, past the transient.

# Conservation equations III



When written in the “flame frame”

$$\rho u = \text{const} = \rho_u s_L \quad (70)$$

$$\frac{\partial}{\partial x} (\rho(u + V_k) Y_k) = \rho_u s_L \frac{\partial Y_k}{\partial x} + \frac{\partial}{\partial x} (\rho V_k Y_k) = \dot{\omega}_k \quad (71)$$

$$\rho_u s_L C_p \frac{\partial T}{\partial x} = \dot{\omega}_T' + \frac{\partial}{\partial x} \left( \lambda \frac{\partial T}{\partial x} \right) - \frac{\partial T}{\partial x} \left( \rho \sum_{k=1}^N C_{p,k} Y_k V_k \right) \quad (72)$$

The equations above are complemented with the equation of state  $\rho = p_0 / RT$  and suitable models for transport properties and kinetics, which are functions of  $(T, Y_1, \dots, Y_M, p_0)$ .

*The equations above are solved numerically with suitable boundary conditions, numerical methods, and arbitrarily complex models for chemistry, thermodynamics, and reactions, yielding the solution to a one-dimensional, unstretched premixed flame.*

# The momentum equation



The momentum equation may be solved (neglecting viscous stresses) to obtain the dynamic pressure field  $p(x)$  across the flame

$$\frac{\partial p}{\partial x} = -\rho u \frac{\partial u}{\partial x} = -\rho_u s_L \frac{\partial u}{\partial x} \quad (73)$$

$$p(x) - p_u = \rho_u s_L (u(x) - s_L) \quad (74)$$

If changes in the molecular mass are neglected,  $\rho_u/\rho = T/T_u$  and one may estimate the pressure difference across a propagating laminar premixed flame

$$p_b - p_u \approx \rho_u s_L^2 (1 - T_b/T_u) \quad (75)$$

As a matter of example, take  $T_b/T_u = 7$ ,  $\rho_u = 1 \text{ kg/m}^3$ , and  $s_L = 0.5 \text{ m/s}$ . Then,  $p_b - p_u = -1.5 \text{ Pa}$ . Hence the pressure jump across flames is  $\mathcal{O}(1) \text{ Pa}$ , ***the effect of which on density may be safely neglected.***

# A useful simplification to the problem



- Only one irreversible reaction:  $\nu_F F + O \rightarrow P$
- Very lean flames, so that  $Y_O \approx const$
- Specific heat is constant:  $C_p = const$
- The fuel's Lewis number is unity:  $Le_F = \lambda / (\rho C_p D_F) = 1$

Under the assumptions above, the reaction rate and heat release rates are

$$\dot{\omega}_F = \dot{\omega}_F(Y_F, T) = \nu_F \rho Y_F A T^n e^{-T_E/T} = B \rho Y_F T^n \exp(-T_E/T) \quad (76)$$

$$\dot{\omega}_T = Q \omega_F \quad (77)$$

where  $B = \nu_F A$  is a modified pre-exponential factor,  $n$  is the temperature exponent,  $T_E$  is the activation temperature, and  $Q$  is the heat released per unit mass of fuel.

# Simplified equations



**Continuity:**  $\rho u = \text{constant} = \rho_u s_L$  (78)

**Species, i.e., fuel:**  $\rho_u s_L \frac{dY_F}{dx} = \frac{d}{dx} \left( \rho D \frac{dY_k}{dx} \right) - \dot{\omega}_F$  (79)

**Energy:**  $\rho_u s_L C_p \frac{dT}{dx} = \frac{d}{dx} \left( \lambda \frac{dT}{dx} \right) + Q \dot{\omega}_F$  (80)

- 3 unknowns:  $s_L$ ,  $Y_F$  and  $T$
- Eq.(78): constant mass flow rate across the flame,  $s_L$  is the flame speed
- Eq.(79): **convection of  $Y_F$  = diffusion of  $Y_F$  + consumption of  $Y_F$**
- Eq.(80): **convection of  $T$  = diffusion of  $T$  + generation of  $T$**
- $Y_F$  and  $T$  obey the same equation

# Equivalence of $Y_F$ and T



Now introduce the “reduced variables”

$$Y = Y_F / Y_F^u \quad \text{and} \quad \Theta = \frac{C_p(T - T_u)}{QY_F^u} = \frac{T - T_u}{T_b - T_u}, \quad (81)$$

The reduced temperature  $\Theta$  is also known as the progress variable and the species equation of fuel and energy equation become:

$$\rho_u s_L \frac{dY}{dx} = \frac{d}{dx} \left( \rho D \frac{dY_k}{dx} \right) - \dot{\omega}_F / Y_F^u \quad (82)$$

$$\rho_u s_L \frac{d\Theta}{dx} = \frac{d}{dx} \left( \frac{\lambda}{C_p} \frac{d\Theta}{dx} \right) + \dot{\omega}_F / Y_F^u \quad (83)$$

Since  $Le = (\lambda / \rho C_p) / D = 1$ , the summation of above equations gives:

$$\rho_u s_L \frac{d}{dx} (Y + \Theta) = \frac{d}{dx} \left[ \rho D \frac{d}{dx} (Y + \Theta) \right] \quad (84)$$

# Equivalence of $Y_F$ and T



$$\rho_u s_L \frac{d}{dx} (Y + \Theta) = \frac{d}{dx} \left[ \rho D \frac{d}{dx} (Y + \Theta) \right] \quad (85)$$

The boundary conditions are  $Y + \Theta = 1$  in both unburnt and burnt gases, so the only solution to Eq.(85) is

$$Y + \Theta = 1 \quad (86)$$

## Some observations

- $Y + \Theta$  is a conserved scalar and is independent of chemistry
- The solution shows the equivalence of fuel mass fraction and temperature
- It also tell us that the fuel species equation and the temperature equation are not independent: we only need to solve one of them

# Reaction rate

Recall that the reaction rate of fuel is:

$$\dot{\omega}_F = \dot{\omega}_F(Y_F, T) = \nu_F \rho Y_F A T^n e^{-T_E/T} = B \rho Y_F T^n \exp(-T_E/T) \quad (87)$$

Now substitute  $Y = 1 - \Theta$  into chemical term of reduced temperature equation:

$$\frac{\dot{\omega}_F(Y_F, T)}{Y_F^u} = B \rho (1 - \Theta)(T_u + \Theta(T_b - T_u))^n \exp\left(-\frac{T_E}{T_u + \Theta(T_b - T_u)}\right) \quad (88)$$

Now define (Poinsot and Veynante, 2005):

$$\alpha = \frac{T_b - T_u}{T_b 0} \quad \text{and} \quad \beta = \alpha T_E / T_b \quad (89)$$

Then Eq. (88) becomes

$$\begin{aligned} \frac{\dot{\omega}_F}{Y_F^u} &= B \rho T^n \exp(-\beta/\alpha) \left[ (1 - \Theta) \exp\left(-\frac{\beta(1 - \Theta)}{1 - \alpha(1 - \Theta)}\right) \right] \\ &= B \rho T^n \exp(-\beta/\alpha) \omega(\Theta; \alpha, \beta). \end{aligned} \quad (90)$$



# Reduced equation



$$\rho_u s_L \frac{d\Theta}{dx} = \frac{d}{dx} \left( \frac{\lambda}{C_p} \frac{d\Theta}{dx} \right) + B\rho T^n \exp(-\beta/\alpha) \omega(\Theta; \alpha, \beta) \quad (91)$$

Define the scaling spatial variable:

$$\xi = \int_0^x \frac{\rho_u s_L C_p}{\lambda} dx \quad (92)$$

Then, the convective and diffusive terms become:

$$\frac{d\Theta}{dx} = \frac{d\Theta}{d\xi} \frac{d\xi}{dx} = \frac{\rho_u s_L C_p}{\lambda} \frac{d\Theta}{d\xi} \quad (93)$$

$$\frac{d}{dx} \left( \frac{\lambda}{C_p} \frac{d\Theta}{dx} \right) = \rho_u s_L \frac{d}{d\xi} \left( \frac{d\Theta}{dx} \right) \frac{d\xi}{dx} = \frac{\rho_u s_L C_p}{\lambda} \frac{d^2\Theta}{d\xi^2} \quad (94)$$

# Reduced flame equation I

The reduced equation for a steady laminar flame is:



$$\frac{d\Theta}{d\xi} = \frac{d^2\Theta}{d\xi^2} + \Lambda\omega(\Theta; \alpha, \beta) \quad (95)$$

where:

$$\Lambda = \frac{B}{\rho_u^2 s_L^2 C_p} (\rho \lambda T^n) \exp(-\beta/\alpha) \quad (96)$$

is the “flame parameter” (note that, by definition,  $B > 0$ ).

- Equation (95) is a second-order ODE with a non-linear reactive term
- If one may assume  $\Lambda \approx \text{const}$ ,  $\Lambda$  plays the role of an unknown parameter
- Three boundary conditions are to be imposed:  $\Theta(0) = 0$ ,  $\Theta(\xi \rightarrow \infty) = 1$ , and  $\Theta'(\xi \rightarrow \infty) = 0$
- In this simple flame model, the flame parameter is a constant if and only if  $\rho \lambda T^n = \text{const}$ , in which case, we may simply let  $\rho \lambda T^n = \rho_u \lambda_u T_u^n$

# Reduced flame equation II



For the sake of simplicity, let  $\rho\lambda T^n = \text{const}$ , which corresponds to assuming the following model for the thermal conductivity  $\lambda$

$$\lambda = \lambda_u \left( \frac{T}{T_u} \right)^{1-n} \quad (97)$$

Then the expression for the flame parameter becomes

$$\Lambda = \frac{\rho\lambda BT^n}{\rho_u^2 s_L^2 C_p} \exp(-\beta/\alpha) = \frac{D_{\text{th},u} B T_u^n}{s_L^2} \exp(-\beta/\alpha) \quad (98)$$

Since  $\Lambda = \Lambda(\alpha, \beta)$  is a function of the user-defined parameters  $\alpha$  and  $\beta$ , it is clear that the laminar flame speed is

$$s_L = (D_{\text{th},u} B T_u^n)^{1/2} [\Lambda(\alpha, \beta)]^{-1/2} \exp(-\beta/2\alpha) \quad (99)$$

# The structure of a premixed flame



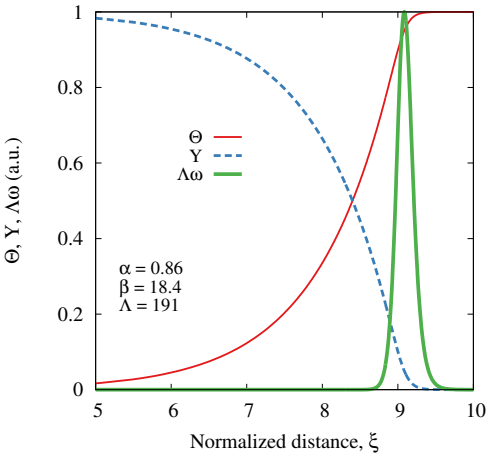
Consider a model flame (Poinsot and Veynante, 2005)

$$\alpha = \frac{T_b - T_u}{T_b} = \frac{2200 - 300}{2200} \approx 0.86$$

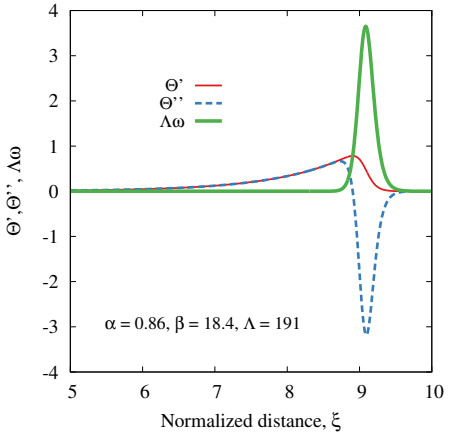
$$\beta = \alpha \frac{375 \times 10^3}{8.314} \frac{1}{2200} \approx 18.4$$

where we let  $E_a = 375 \text{ kJ/mol}$  as a reasonable value for the activation energy.

Upon solving the ODE in  $\xi \in [0, 10]$ , the flame parameter is  $\Lambda = 191$ .



# Balances in a premixed flame



- Recall that the ODE is

$$\Theta' = \Theta'' + \Lambda\omega(\Theta; \alpha, \beta)$$

- The distribution of the convective ( $\Theta'$ ), diffusive ( $\Theta''$ ), and reactive terms ( $\Lambda\omega$ ) indicates the existence of two regions.
- In the thermal layer ahead of the flame,  $\Theta' = \Theta''$  and  $\omega \approx 0$ .
- In the reaction zone,  $-\Theta'' = \Lambda\omega$ .

Notice that the reaction zone is much smaller than the thermal layer, where “heat” diffuses ahead of the flame.

# Flame parameter



Because the flame parameter is a unique function of  $(\alpha, \beta)$ , one may seek approximate functional representations. Two are available:

- Based on the solution by Zeldovich, Frank-Kamenetskii, and von Karman (ZFK)

$$\Lambda = \frac{1}{2}\beta^2 \quad (100)$$

- Based on the solution by Williams (Williams, 1994)

$$\Lambda = \frac{1}{2}\beta^2 \left[ 1 + \frac{2}{\beta}(3\alpha - 1.344) \right] \quad (101)$$

which is a second-order correction to the ZFK.

For  $\alpha = 0.86$  and  $\beta = 18.4$ , one obtains  $\Lambda = 192$ , which is very close to the value  $\Lambda = 191$  obtained via direct integration.

# Interpretation



Let us consider the simple ZFK expression for  $\Lambda$  and rewrite Eq. (99) for the laminar flame speed  $s_L$ :

$$s_L = \frac{1}{\beta} \exp(-\beta/2\alpha) (2D_{\text{th},u} |B| T_u^n)^{1/2} \quad (102)$$

*It is clear that  $s_L$  is a parameter of the solution. Often, it is said that  $s_L$  is an “eigenvalue” of the problem. This concept applies to simplified laminar flame models as well as to complex kinetics.*

A good question is “what do we do with this simple model and what can be learnt?”

# Lessons to be learnt



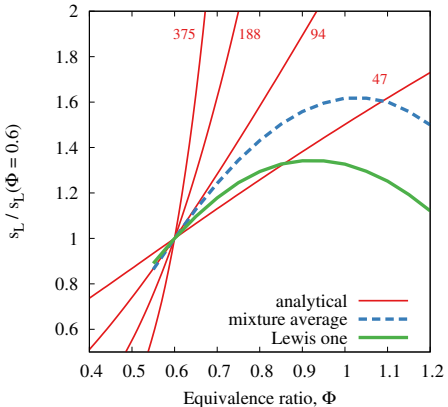
Let us begin by writing down how the parameters  $\alpha$  and  $\beta$  relate to the equivalence ratio  $\Phi$ .

Firstly, recall that  $Y_F^u = (\Phi/s)/(1 + \Phi/s)$ . Secondly let  $T_b = T_u + QY_F^u/C_p$ , which seems a reasonable simplification for lean flames. Also, consider flames with  $T_u = 800$  K.

For methane,  $Q = 50.1$  MJ/kg and  $C_p = 1.0$  kJ/kg-K for air, which again is the main constituent of lean flames.

Based on the definitions,  $\alpha = (T_b - T_u)/T_b = \alpha(\Phi)$  and  $\beta = \alpha T_a/T_b = \beta(\Phi)$ , where  $T_a = E_a/R$  is the activation temperature.

# The variation of $s_L$ with $\Phi$



The data is shown normalized by the flame speed at  $\Phi = 0.6$ , assuming that  $|B| T_u^n D_{th,u}$  remains constant as  $\Phi$  varies.

The analytical solution is shown for various values of the activation energy  $E_a = \{375, 188, 94, 47\}$  kJ/mol and compared to PREMIX solutions.

The rate of change of  $s_L$  with respect to  $\Phi$  is a strong function of the “activation energy” of the single-step reaction, further suggesting that  $E_a = E_a(\Phi)$ .

*The plot above shows unequivocally that complex chemistry is responsible for the variation of  $s_L$  with  $\Phi$  and that one may not use an irreversible step reaction with constant parameters for all  $\Phi$ .*

# Laminar Premixed Flames - PREMIX



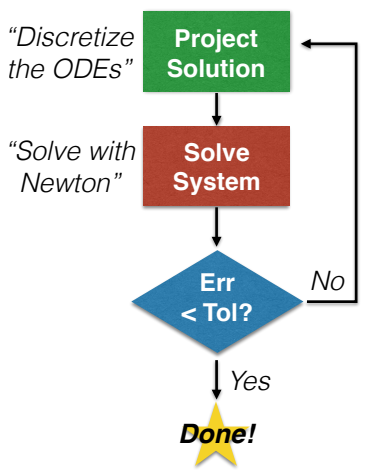
PREMIX is a solver for one-dimensional, unstretched, premixed flames with support for realistic thermodynamics, transport and kinetics data.

It is part of the CHEMKIN package and relies on a boundary value problem solver to recover the laminar flame speed as an “eigenvalue” to the problem.

## Key features

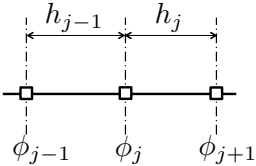
- Handles complex chemistry, transport, and thermodynamics
- Solves for the one-dimensional steady laminar flame
- Provides the “laminar flame speed”  $s_L$  and distribution of temperature, and species mass fractions as part of the solution

# Solution strategy



- Once discretized on an appropriate grid, the equations are solved as a system of nonlinear equations
- The size of the system is  $Q = N \times (M + 1 + 1)$ , where  $Q$  is the number of unknowns,  $N$  is the number of grid points and  $M$  is the number of species. E.g., methane/air flame consists of about  $Q = 120 \times (53 + 1 + 1) = 6600$  unknowns.
- The method of choice for the solution of the nonlinear system of equations is modified Newton.
- Modified Newton requires (a) Jacobians of the system ( $\mathcal{O}(Q^2)$ ); (b) solution of linear systems ( $\mathcal{O}(Q^3)$ );

# Discrete form of the convective term



On the convective terms the user has the choice of using either first order windward differences:

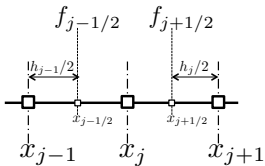
$$\left( (\rho u) \frac{\partial \phi}{\partial x} \right)_j \approx (\rho u)_j \left( \frac{\phi_j - \phi_{j-1}}{x_j - x_{j-1}} \right) \quad (103)$$

or central differences :

$$\left( \rho u \frac{\partial \phi}{\partial x} \right)_j \approx (\rho u)_j \left( \frac{h_{j-1}}{h_j(h_j + h_{j-1})} \phi_{j+1} + \frac{h_j - h_{j-1}}{h_j h_{j-1}} \phi_j - \frac{h_j}{h_{j-1}(h_j + h_{j-1})} \phi_{j-1} \right) \quad (104)$$

$\phi$  can be  $T$  or  $Y_k$ . The index  $j$  refers to the mesh point and  $h_j = x_{j+1} - x_j$ .

# Discrete form of the diffusive term



The second derivative term in the energy equation is approximated by:

$$\frac{\partial}{\partial x} \left( \lambda \frac{\partial T}{\partial x} \right)_j \approx \left( \frac{2}{x_{j+1} - x_{j-1}} \right) \left[ \lambda \left( \frac{T_{j+1} - T_j}{x_{j+1} - x_j} \right) - \lambda \left( \frac{T_j - T_{j-1}}{x_j - x_{j-1}} \right) \right] \quad (105)$$

The coefficients  $\lambda$  (at  $j \pm 1/2$ ) are evaluated using the averages of the dependent variables between mesh points.

The species diffusion term is evaluated with the following difference approximation:

$$\frac{\partial}{\partial x} (\rho Y_k V_k) \approx \frac{f_{j+1/2} - f_{j-1/2}}{x_{j+1/2} - x_{j-1/2}} \approx \frac{(\rho Y_k V_k)_{j+1/2} - (\rho Y_k V_k)_{j-1/2}}{x_{j+1/2} - x_{j-1/2}} \quad (106)$$

# Boundary conditions & flame speed “eigenvalue”

## Flame speed “eigenvalue”

In order to solve for the flame “eigenvalue”  $\rho s_L$ , an additional first order ODE is added to the system of equations, and discretized

$$\frac{d\rho u}{dx} = 0 \quad \text{discretized as} \quad \frac{(\rho u)_j - (\rho u)_{j-1}}{x_j - x_{j-1}} = 0 \quad (107)$$

## Boundary conditions

At the cold boundary we specify the mass flux fractions and the temperature, i.e. we solve:

$$\epsilon_{k,1} - Y_{k,1} - \left( \frac{\rho Y_k V_k}{\rho u} \right)_{j=\frac{1}{2}} = 0 \quad (108)$$

$$T_1 - T_b = 0 \quad (109)$$

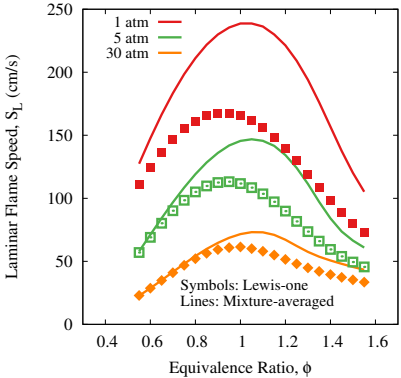
where  $\epsilon_{k,1}$  is the inlet reactant fraction of the  $k^{th}$  species and  $T_b$  is the specified burner temperature. At the hot boundary we specify that all gradients vanish:

$$\frac{Y_{k,J} - Y_{k,J-1}}{x_J - x_{J-1}} = 0 \quad \frac{T_J - T_{J-1}}{x_J - x_{J-1}} = 0 \quad (110)$$

# Laminar Flame speeds from PREMIX



- Flame speeds range from 100 to 250 cm/s at atmospheric pressure
- $s_L$  is maximum for  $\Phi \approx 1$ , increasing with  $\Phi$  for  $\Phi < 1$  (lean flames)
- $s_L$  decreases with increasing pressure (more later).
- Mixture averaged transport results in larger flame speeds
- The closure for the diffusive velocity has a larger effect for richer mixtures and at near atmospheric pressures

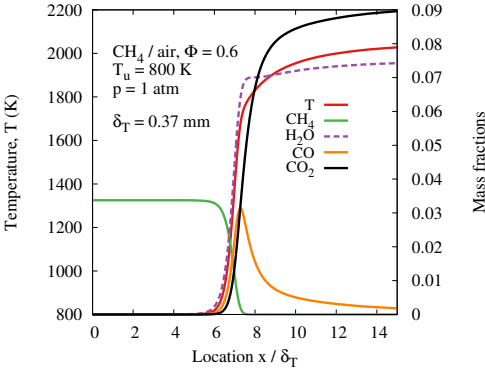


$s_L$  for methane/air at  $T_u = 800$  K and various pressures. Both mixture-averaged and Lewis unity models are shown.

# Flame structure: major species



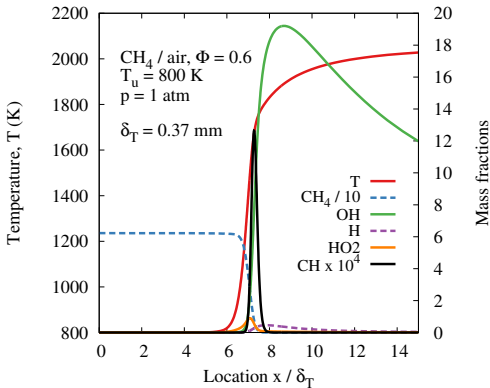
- The premixed flame appears as a “thin” interface (about 0.5 mm at those conditions) separating the unburnt and burnt gases
- The methane fuel  $\text{CH}_4$  is consumed ahead of the flame front
- The flame front is identified by a rapid rise in temperature and product species, such as  $\text{H}_2\text{O}$
- $\text{CO}$  increases and then decreases in the burnt region of the flame as it is oxidizer to  $\text{CO}_2$



Various species and temperature across a methane/air ( $\Phi = 0.6$ ) at  $T_u = 800 \text{ K}$  and 1 atm. The thermal flame thickness is  $\delta_T = 0.37 \text{ mm}$ .

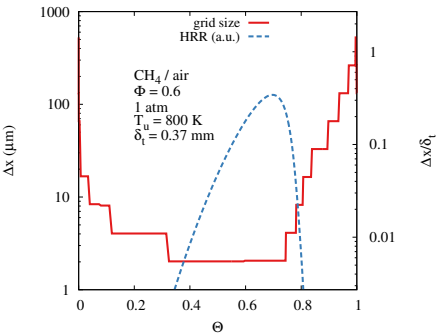
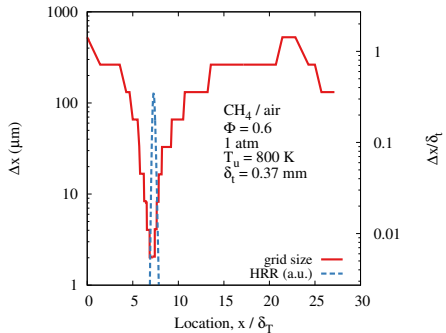
# Flame structure: intermediate and radical species

- Reactants are consumed ahead of the flame and are turned into intermediate species prior to products forming
- Notable intermediates include CO, carbon monoxide
- Many intermediates are radical species such as  $\text{HO}_2$  and  $\text{CH}$ , which are formed and consumed "inside the reaction zone" with very rapid time scales.
- Other radicals, such as OH persist in the "burnt flame region" over long distances



$s_L$  for methane/air ( $\Phi = 0.6$ ) at  $T_u = 800 \text{ K}$  and 1 atm. The thermal flame thickness is  $\delta_T = 0.37 \text{ mm}$ .

# Grid refinement and spacing

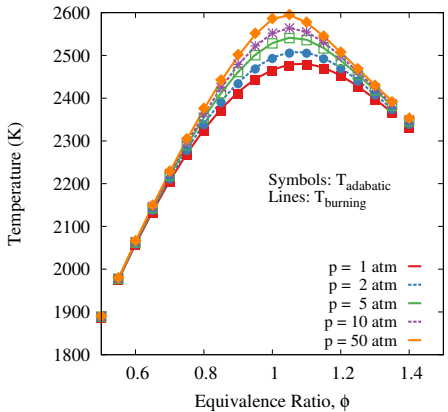


The reaction zone poses the most strict requirements on grid size  
 $\Delta x/\delta_T \approx 1/100$  with physical size  $\Delta x \approx 2$  μm.

Outside of the reaction zone (defined as  $0.3 \leq \Theta \leq 0.8$ ),  $\Delta x \geq 100$  μm is acceptable.

*Adaptive mesh refinement is a useful strategy when simulating premixed flames.*

# Adiabatic temperature and $T_b$



If enthalpy is conserved,  $T_{\text{ad}}$ , the adiabatic flame temperature, for the reactants matches the flame burnt temperature  $T_b$ .

Shown on the left, is the equilibrium temperature at constant enthalpy and pressure ( $T_{\text{ad}}$ ) as computed from thermodynamic equilibrium. The results for the burnt temperature from PREMIX are shown also.

*Those comparisons are very useful during development for the sake of code validation.*

# Reducing mechanisms: introduction



For a given fuel, e.g., methane, there exist many “combustion mechanisms” of increasing complexity (measured as number of species and reactions).

A good question is

*Just how “complex” does the mechanism need to be to capture the “desired” features of a premixed flame?*

This question is deceptively simple and the answer depends on (a) conditions of interest and (b) desired features.

The answer has tremendous implications for numerical combustion as “costs” increase with the number of species and reactions.

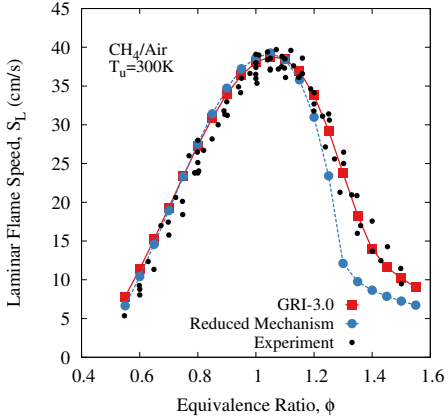
# Skeletal mechanism for lean premixed methane/air flames



We set forth the goal of “reducing” the detailed GRIMech 3.0 mechanism to generate a subset of species (and related reactions) capable of describing lean methane/air flames.

- The reduction was accomplished through the sequential application of directed relation graph (DRG), sensitivity analysis over the GRI3.0 detailed mechanism.
- To assure minimal loss of kinetic information, the reduction was conducted by sampling a set of reaction states from autoignition application.
- The reaction states were sampled under atmospheric pressure, equivalence ratio 0.8 for the intended lean combustion, and initial temperature of 1000 K.
- The final “skeletal” mechanism contains 16 species and 73 reactions (against the 53 species of GRIMech 3.0)

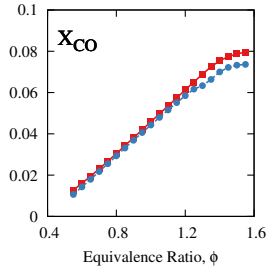
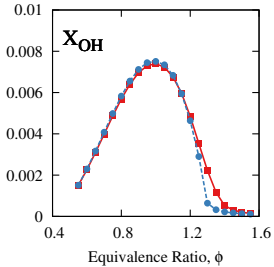
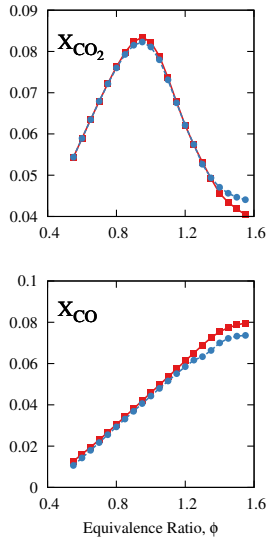
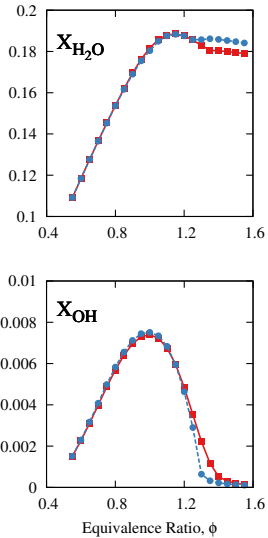
# $s_L$ : skeletal vs. detailed



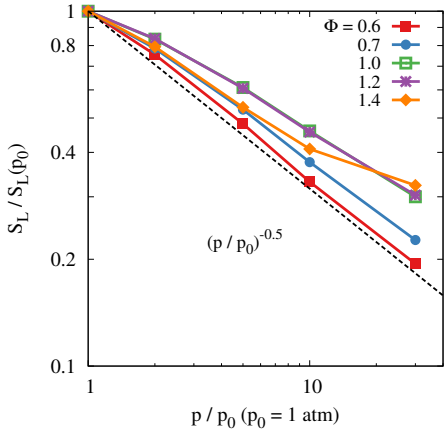
- We consider the laminar flame speed at 1 atm for  $T_u = 300\text{ K}$  reactants
- Validation is performed with PREMIX code with mixture-averaged transport
- The laminar flame speed is compared with experimental data from Vagelopoulos (1994, 1998), de Goey (2004) and Tahtouh (2009)

*It is clear that, on the lean side of the curve, the agreement is exceptional, while some discrepancies exist on the rich side, highlighting the effect of more “complex chemistry” that was removed.*

# Species: skeletal vs. detailed



# Pressure scaling of $s_L$



For lean methane/air mixtures ( $\Phi \approx 0.6$ ),  $s_L$  decreases with pressure as  $p^{-0.5}$ .

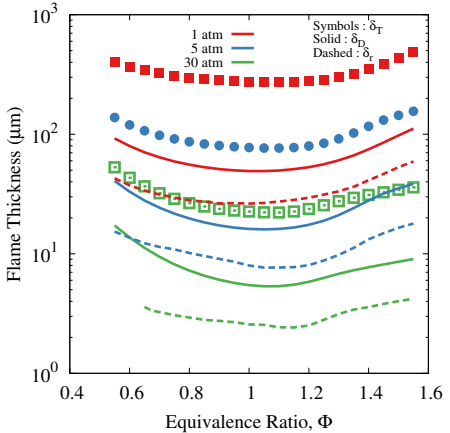
Recall that the single-step irreversible reaction model gives

$$s_L = \frac{1}{\beta} \exp(-\beta/2\alpha) (2D_{th,u} |B| T_u^n)^{1/2}$$

Under the assumption that if  $\Phi = const$ , one has  $\beta \approx const$ ,  $\alpha \approx const$  and  $B \approx const$ , it is clear that  $s_L \propto D_{th,u}^{1/2} \propto p^{-1/2}$

*This interpretation is over-simplistic and neglects pressure effects on chemistry, which manifest themselves as  $\Phi$  increases, but provides a reasonable approximation for lean flames.*

# Flame thickness and its pressure scaling



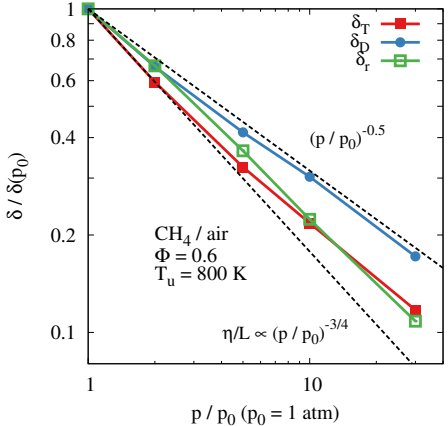
- Thickness from  $T(x)$ :  
$$\delta_T = (T_b - T_u)/\max\{|dT/dx|\}$$
- Diffusive thickness:  $\delta_D = D_{\text{th}}/s_L$
- Thickness of the reaction zone, based on 0.1 max(HRR):  $\delta_r$

Depending on the definition, the “flame thickness” may vary by up to one order of magnitude:  $\delta_r < \delta_D \ll \delta_T$ .

The ratios among the various “thicknesses” stays constant as pressure increases.

*Resolution requirements should be based on a carefull assessment of the dependence of the flame speed and flame structure on the size of the computation grid, **not only** on “classical scaling” arguments!*

# Scaling of thickness with pressure



Consider lean, preheated methane/air flames:  $\Phi = 0.6$ ,  $T_u = 800$  K

The flame thickness scales between  $-3/4$  to  $-1/2$  with pressure, depending on the definition.

From a computational perspective, those scaling have important implications, namely grid resolution

The  $(p/p_0)^{-3/4}$  scaling illustrates the effect of pressure on the Kolmogorov scale ( $\eta/L \propto Re^{-3/4}$  with  $Re \propto p^{-1}$ ).



# Laminar nonpremixed flames

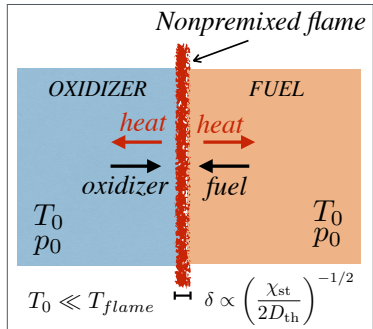
# Introduction



*"Nonpremixed flames constitute a specific class of problems where fuel and oxidizer are not mixed prior to reacting.*

*[...] for those flames, mixing must bring reactants into the reaction zone fast enough for combustion to proceed" (Poinsot and Veynante, 2005).*

Two boundaries must be considered:  
oxidizer on the left and fuel on the right.



*Temperature is maximum in the reaction zone, which is confined to a region where the mixture fraction is stoichiometric,  $Z \approx Z_{st}$ . Mixing results in the diffusion of heat, products (resp. reactants) out of (resp. into) the reactions zone. The thickness of the flame is controlled by the gradient of the mixing layer*

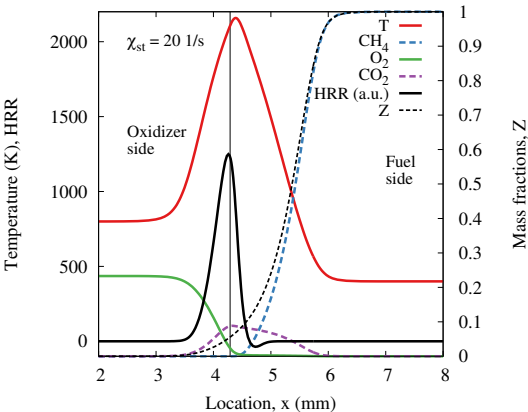
$$\delta \propto \chi_{st}^{-1/2} = (2\mathcal{D}|\nabla Z|^2)^{-1/2}.$$

# Structure of nonpremixed flame



Let us consider a strained methane/air nonpremixed flame at 1 atm,  $\chi_{st} = 20 \text{ l/s}$  obtained in a “counterflow” configuration.

- Notice that fuel and oxidizer diffuse into the reaction zone
- The temperature is maximum in the reaction zone at the location of  $Z = Z_{st}$
- The flame structure is steady only when strain is applied (i.e., in a counterflow configuration)
- Nonpremixed flames do not exhibit a reference “speed” nor a reference “thickness”

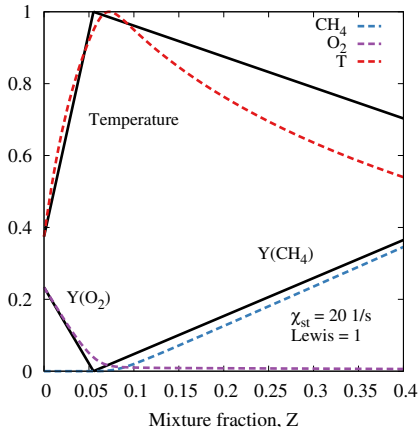


# The Burke-Schumann flame structure

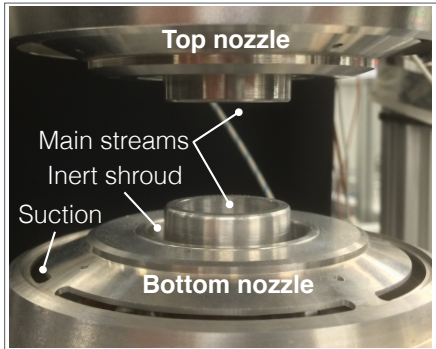


In the limit of irreversible, infinitely fast chemistry, the mass fractions of oxidizer, fuel and products and the temperature are functions of mixture fraction  $Z$ .

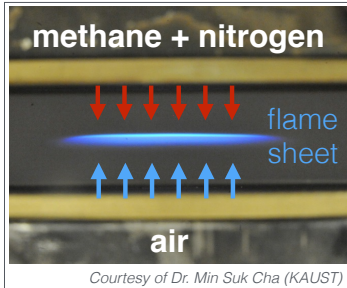
- A methane/air, 1 atm counterflow flame ( $Z_{st} = 0.055$ ) with finite rate chemistry is compared to the Burke-Schumann solution (thick black lines).
- Oxygen “leaks” into the fuel side
- The location of peak temperature shifts to the fuel side
- Methane “disappears” (i.e., decomposes) before reaching the flame sheet at  $Z = Z_{st}$
- The temperature on the fuel side is significantly lower than B-S (mixing).



# The counterflow burner



Counterflow setup at the Reactive Flow Modeling Laboratory  
at KAUST  
<http://flow.kaust.edu.sa>



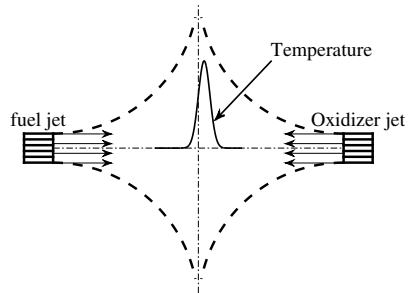
Courtesy of Dr. Min Suk Cha (KAUST)

The counterflow setup is used for premixed and nonpremixed flames by many research groups: Law (Princeton), Chung (KAUST), Chelliah (U Virginia), Egolfopoulos (USC), Gomez (Yale), Peters/Pitsch (RWTH Aachen), Seshadri/Williams (UCSD), and Mastorakos (Cambridge).

# The one-dimensional counterflow flame

The laminar one-dimensional counterflow flame configuration consists in a boundary value problem with parameter and describes the flow field in between opposing reactive jets.

- Counterflow flames are used to investigate ignition, extinction, and structure of nonpremixed flames
- The one-dimensional counterflow flame is used to develop closure models for turbulent nonpremixed combustion
- Often numerical solutions are compared to experiments
- Computations are numerically affordable

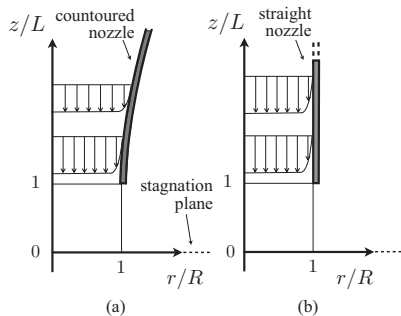


# Problem definition



The configuration is uniquely identified by:

- $H = 2L$ : nozzle separation distance
- $T_{f,o}$ : streams' temperature
- $\mathbf{Y}_{f,o}$ : streams' compositions
- $u_{f,o}$ : streams' bulk velocities
- $p$ : pressure



The (fuel side) Reynolds number is defined as:  $Re_f = u_f L / \nu_f$ , where  $L$  is the half separation distance

# Streamfunction formulation and quasi-one-dimensional solution



## The streamfunction

In cylindrical coordinates, let's assume that the following stream function

$$\psi(z, r) = r^2 U(z) \quad (111)$$

is an adequate description of the flow field, where  $z$  and  $r$  are the axial and radial coordinates respectively.

Given the definition of a streamfunction in cylindrical coordinates, recall that

$$\frac{\partial \psi}{\partial r} = r\rho u = 2rU, \quad \frac{\partial \psi}{\partial z} = r\rho v = -r^2 \frac{dU}{dz} \quad (112)$$

so that the continuity equation is satisfied

$$\frac{\partial}{\partial x} (r\rho u) + \frac{\partial}{\partial r} (r\rho v) = 0. \quad (113)$$

# Formulation



## Radial and axial momentum

The expressions of the velocity components are substituted in the momentum equations (radial and axial)

$$\frac{\partial p}{\partial z} = -4U \frac{d}{dz} \left( \frac{U}{\rho} \right) - 2\mu \frac{d}{dz} \left( \frac{1}{\rho} \frac{dU}{dz} \right) + \frac{4}{3} \frac{d}{dz} \left[ 2\mu \frac{d}{dz} \left( \frac{U}{\rho} \right) + \nu \frac{dU}{dz} \right] \quad (114)$$

$$\frac{1}{r} \frac{\partial p}{\partial r} = \frac{d}{dz} \left( \frac{2U}{\rho} \frac{dU}{dz} \right) - \frac{3}{\rho} \left( \frac{dU}{dz} \right)^2 - \frac{d}{dz} \left[ \mu \frac{d}{dz} \left( \frac{1}{\rho} \frac{dU}{dz} \right) \right] \quad (115)$$

Both terms  $1/r(\partial p/\partial r)$  and  $\partial p/\partial z$  are functions of  $z$ , hence

$$\frac{\partial}{\partial z} \left( \frac{1}{r} \frac{\partial p}{\partial r} \right) = \frac{1}{r} \frac{\partial}{\partial r} \left( \frac{\partial p}{\partial z} \right) = 0 \quad \Rightarrow \quad \boxed{\frac{1}{r} \left( \frac{\partial p}{\partial r} \right) = H = \text{const}} \quad (116)$$

where  $H$  is called the *radial pressure-gradient eigenvalue*.

# Governing equations



Based on the derivations above, one may formulate the following system of  $2 + 1 + N$  equations in  $2 + 1 + N$  unknowns ( $U, G, T, Y_k$  with  $k = 1, \dots, N$ ) below:

$$\frac{dU}{dz} - G = 0 \quad (117)$$

$$\frac{d}{dz} \left[ \mu \frac{d}{dz} \left( \frac{G}{\rho} \right) \right] - 2 \frac{d}{dz} \left( \frac{UG}{\rho} \right) + \frac{3}{\rho} G^2 + H = 0 \quad (118)$$

$$2U \frac{dT}{dz} - \frac{1}{C_p} \frac{\partial}{\partial z} \left( \lambda \frac{dT}{dz} \right) + \frac{\rho}{C_p} \sum_{k=1}^K Y_k C_{pk} V_k \frac{dT}{dz} + \frac{1}{C_p} \sum_{k=1}^K h_k \dot{\omega}_k = 0 \quad (119)$$

$$2U \frac{dY_k}{dz} + \frac{d}{dz} (\rho Y_k V_k) - W_k \dot{\omega}_k = 0 \quad (120)$$

The system of equations is complemented by the equation of state, transport and thermodynamic models and expressions for the reaction rates.

*Note that  $H$  is a “parameter”, which is part of the solution.*

# Boundary conditions



The system of equations above are solved in the domain  $z \in [-L, L]$ .

## Inlet velocities

Inlet velocities are prescribed by:

$$U(-L) = \frac{\rho_L u_L}{2} \quad \text{and} \quad U(L) = \frac{\rho_R u_R}{2}. \quad (121)$$

The radial inlet velocity ( $\rho v = -rdU/dz$ ) is prescribed (through continuity) by setting  $G$  at the inlet. One reasonable choice (but **only a “choice”**) is

$$G(\pm L) = \frac{dU}{dz} = 0, \quad (122)$$

which corresponds to  $v = 0$  at the inlets.

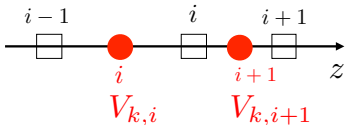
## Inlet scalars

Temperatures ( $T_o$  and  $T_f$ ) and scalars mass fractions ( $\mathbf{Y}_o$  and  $\mathbf{Y}_f$ ) are prescribed at each inlet.

# Discretization



$$U_i, G_i, T_i, Y_{k,i}$$



- Stream function, temperature, and the mass fraction of species are discretized on a cell-centered grid.
- Diffusion velocities are discretized on the mid-points.

$$2U_i \frac{Y_{k,i} - Y_{k,i-1}}{Z_i - Z_{i-1}} + \frac{\rho_{i+1/2} Y_{k,i+1/2} V_{k,i+1} - \rho_i Y_{k,i-1/2} V_{k,i}}{Z_{i+1/2} - Z_{i-1/2}} - W_k \dot{\omega}_{k,i} = 0, \quad (123)$$

# Some comments

## Boundary conditions



- The equation for  $G$  is first-order; the equation for  $U$  is second-order; the equations for  $T$  and  $Y_k$  are second-order.
- While two BCs may be specified for each of  $T$  and  $U$ , we are prescribing **four** BCs for  $G$  and  $U$  ( $U(\pm L)$  and  $G(\pm L)$ ).
- *Why is this the case? Recall the parameter  $H = \text{const}$ , which can be interpreted as an additional equation  $dH/dz = 0$  (as it is actually implemented in discrete form)*

## Solution method

- The problem is again a boundary value problem with parameter. Once discretized, the problem is solved as a non-linear system of equations (Newton's method).
- The algorithm alternates between (a) re-gridding and (b) solving the system
- The cost scales with  $\mathcal{O}(Q^3)$  where  $Q = P \times (3 + N)$ , where  $P$  is the number of points and  $N$  is the number of species

# A model flame



We shall consider a model counterflow flame

- Background pressure is 1 atm
- Oxidizer is air at 800 K ( $\rho_o = 0.4395 \text{ kg/m}^3$  and  $\nu_o = 8.4203 \times 10^{-5} \text{ m}^2/\text{s}$ )
- Fuel is methane at 400 K ( $\rho_f = 0.4888 \text{ kg/m}^3$  and  $\nu_o = 2.9548 \times 10^{-5} \text{ m}^2/\text{s}$ )
- Separation distances are  $H = \{1.5, 1.75, 2\} \text{ cm}$
- Velocities are chosen so that  $20 \leq K \leq 2000 \text{ 1/s}$ , where  $K$  is a characteristic “strain rate” defined as

$$K = \frac{u_f}{H} \left( 1 + \sqrt{\frac{\rho_o}{\rho_f}} \frac{u_o}{u_f} \right) \quad (\text{Williams and Seshadri}), \quad (124)$$

$$u_f = K \frac{H}{2} \quad \text{and} \quad u_o = K \sqrt{\frac{\rho_f}{\rho_o}} \frac{H}{2}. \quad (125)$$

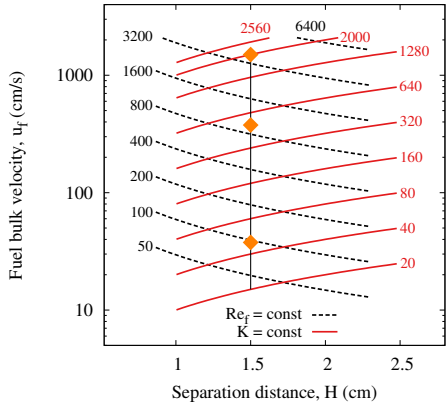
Hence, at constant separation  $H$ , velocities are proportional to strain  $K$ .

# The parameter space of the counterflow

Eq. (124) indicates that one may chose a suitable combination of  $H$  and  $u_{f,o}$  to obtain a desired  $K$ .

For every choice of  $H$  and  $u_{f,o}$  at constant  $K$ ,  $Re_f$  changes.

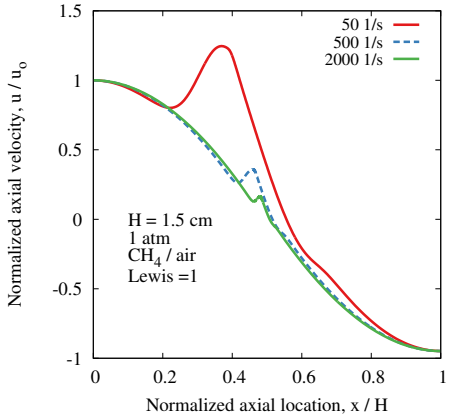
There exist a parameter space  $(H, u_f)$  where a “one-dimensional” counterflow simulation lies for the streams described on the previous slide.



It is clear that as  $u_f$  increases at constant  $H$ ,  $Re_f$  increases with  $K$ .

Note that the symbols along the  $H = 1.5$  cm line correspond to selected case we will explore shortly.

# Velocity distribution at varying $K$



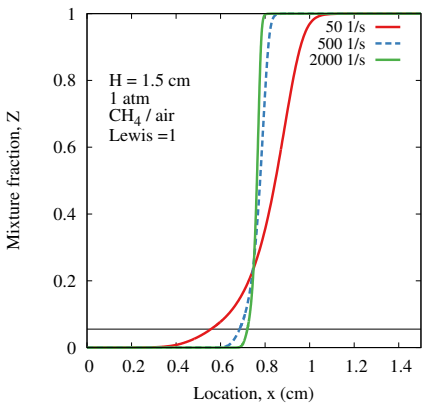
The (normalized) velocity field is shown for  $K = \{50, 500, 2000\}$ .

Notice the sudden increase and decrease of  $u$ , which is due to the presence of the flame and changes in density.

Outside of the “flame”, the normalized velocity is undisturbed and identical to a non-reactive case and largely **independent of  $\text{Re}$  and  $\text{Da} = (K\tau_{\text{rxn}})^{-1}$** .

As  $K$  (and  $\text{Re}$ ) increases at constant  $H$ , the flame is confined to a smaller and smaller region of size  $\delta \ll H$ .

# Mixing field: $Z$



Flames are confined to a narrow region of suitable values of mixture fraction around  $Z = Z_{\text{st}}$ .

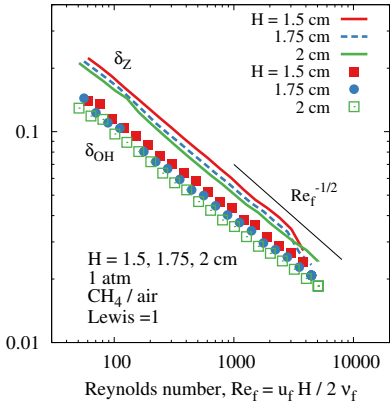
As  $K$  (and  $\text{Re}$ ) increases, the mixing layer between the fuel and oxidizer streams becomes thinner and thinner.

Thus, driven by the thinning of the mixing layer, the nonpremixed flame becomes thinner also.

# Mixing and flame fields: $\delta_Z$ and $\delta_{OH}$



Normalized thickness,  $\delta / H$



The thickness of the mixing layer is defined as

$$\delta_Z = 1 / \max\{dZ/dx\} \quad (126)$$

The thickness of the OH layer (peak to 5%) is also measured and shown as  $\delta_{OH}$ .

It is clear that  $\delta_Z/H$  and  $\delta_{OH}/H$  scale as  $Re_f^{-1/2}$ .

*The result  $\delta_Z/H \propto Re_f^{-1/2}$  is expected and implies that the flame does **not** affect mixing. The result  $\delta_{OH}/H$  implies that the reaction zone thickness is controlled by mixing.*

# Mixing field: $\chi$



The scalar dissipation rate is defined as

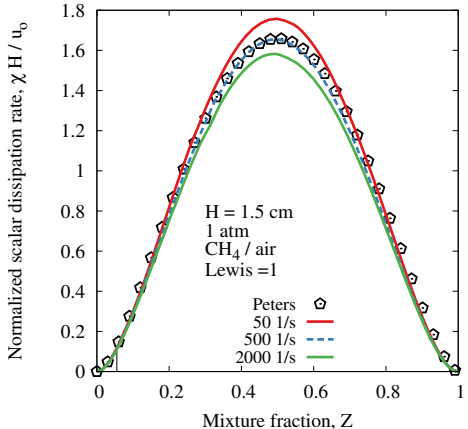
$$\chi = 2\mathcal{D}|\nabla Z|^2 \quad (127)$$

and has units of 1/s.

Here we show the normalized scalar dissipation rate  $\chi H / u_0$  for the three cases  $K = \{50, 500, 2000\}$  1/s.

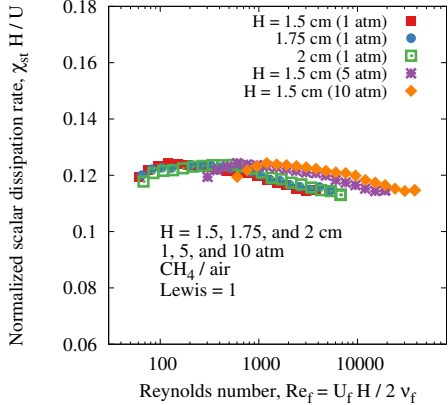
The analytical expression proposed by Peters is

$$\chi(Z) = C \exp\{-2(\text{erfc}^{-1}(2Z))^2\}. \quad (128)$$



*Clearly, the scalar dissipation rate  $\chi(Z)$  is symmetric around  $Z = 0.5$  (although  $Z$  is not, due to  $\mathcal{D} = \mathcal{D}(T)$ ) The expression proposed by Peters works very well.*

# Dependence of $\chi_{\text{st}} H / u_o$ on Re



The scalar dissipation rate at  $Z = Z_{\text{st}}$  is of fundamental importance as it describes the mixing near the reaction zone of the nonpremixed flame.

Here we consider flames with various separations ( $H = \{1.5, 1.75, 2\} \text{ cm}$ ) and pressures ( $p = \{1, 5, 10\} \text{ atm}$ ) over a range of strain rates  $20 < K < 2000 \text{ 1/s}$

The scalar dissipation rate is plotted normalized by the quantity  $u_o/H$  versus  $Re_f$ .

*Clearly,  $\chi_{\text{st}}$  can be made to “collapse” when rescaled by  $K \propto u_o/H$  for various values of  $K$ , geometries, and pressures. Moreover, the normalized  $\chi H / u_o$  is largely constant ( $\approx 0.12$ ) and independent of the Reynolds number.*

# Extinguishing counterflow flames



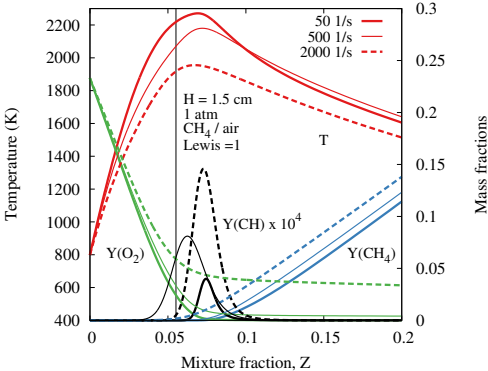
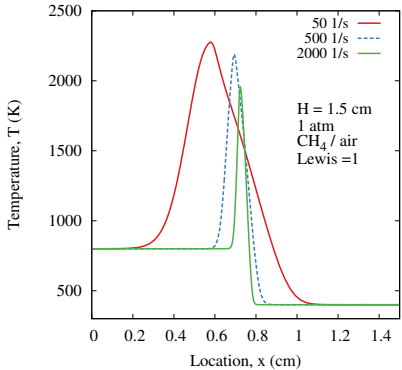
We have shown above that  $K$  controls the thickness of the mixing layer. Largely, this process is not affected by the presence of a flame and occurs as in nonreactive mixing layers.

Next, we are interested in investigating the effect of increasing  $K$  on the nonpremixed flame. As we shall see, as  $K$  increases the peak heat release rate in the reaction zone of the flame increases (as mixing rates increase), **up to a point**.

As  $K$  is increased further, the **flame extinguishes**.

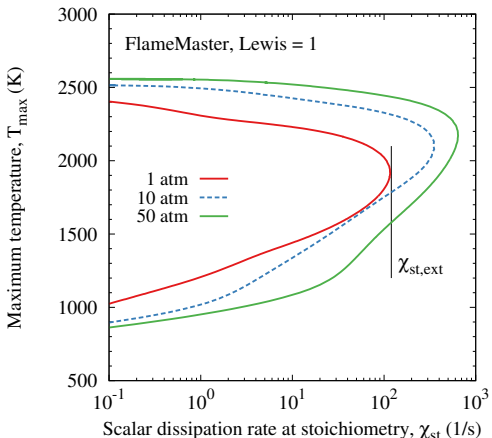
*Since the extinction process is intimately connected with the balance between mixing and reactions, finite rate chemistry effects are key and motivate the usage of one-dimensional counterflow codes.*

# Straining a nonpremixed flame



As the strain rate  $K$  increases, (a) the peak temperature decreases; (b)  $\text{O}_2$  leaks on the fuel side; (c) the peak heat release rate (here quantified by  $Y(\text{CH})$ ) increases; while (d) the extent of the reaction zone in  $Z$ -space (i.e.,  $\Delta Z_{rxn}$ ) remains  $\approx const.$

# The “S-shaped curve”



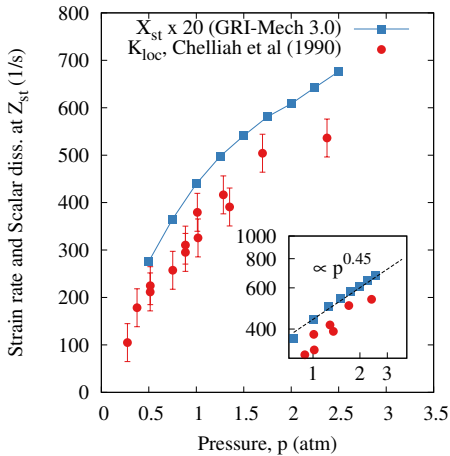
Here we consider three nonpremixed methane/air flames at 1, 10 and 50 atm.

The maximum temperature in the flame is plotted as a function of the scalar dissipation rate at stoichiometry,  $\chi_{st}$ .

As  $\chi_{st}$  increases (due to  $K$  increasing),  $T_{\max}$  decreases, until a flame can no longer be sustained, i.e. extinction occurs at  $\chi_{st,ext}$ .

At 1 atm,  $\chi_{st,ext} \approx 100$  1/s, while as shown,  $\chi_{st,ext}$  increases with pressure, i.e., nonpremixed flames become “more resilient” to extinction with increasing pressure

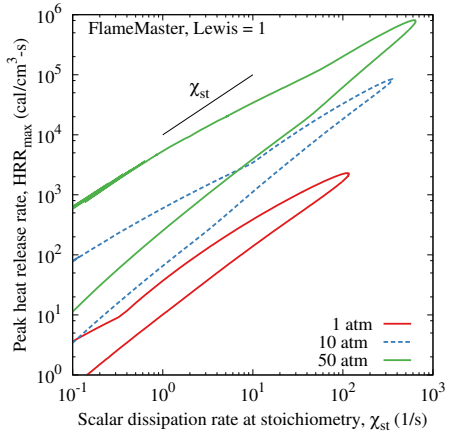
# Pressure scaling of extinction dissipation rate in pure methane flames



Local strain rates  $K_{loc}$  on the oxidizer side of the flame at extinction for methane/air from Chelliah et al. (1990). (solid squares with  $\pm 40$  1/s error bars).

The pressure scaling  $p^{0.45}$  proposed by Chelliah et al. is recovered for the range  $1 < p < 2.25$  atm.

# Heat release rate and rate of mixing



In nonpremixed flames, mixing is the “rate limiting” process as oxidizer and fuel must to mix prior to reacting.

As shown by Peters and Bilger, reactions proceed (and heat is released) only as fast as mixing occurs, implying that  $HRR_{max} \propto \chi_{st}$ .

This important result can be shown analytically with simplified chemistry and is here recovered in the limit of finite rate chemistry and complex transport/thermodynamics.

*Note that (a)  $HRR_{max} \propto \chi_{st}$  only until the flame extinguishes and (b) the peak heat release rate increases with pressure.*



# Zero-dimensional reactors

# Introduction



Just like one-dimensional flames, the “zero-dimensional reactor” is a fundamental configuration in numerical combustion.

It consists of a reactive system with pressure  $p(t)$ , temperature  $T(t)$ , composition  $(\mathbf{Y}(t))$  and volume  $V(t)$ .

The system is surrounded by an impermeable (no mass transfer) and adiabatic (no heat transfer) walls.

## Applications

- A model for shock-tubes and kinetics studies
- A tool for Computational Fluid Dynamics in the context of operator splitting (more later)
- A model for studying the properties of chemical kinetics networks

*Impermeable & adiabatic walls*

$V(t)$   $\mathbf{Y}(t)$   
 $T(t)$   $p(t)$

# Basic equations



- $y_k$ ,  $x_k$ , and  $c_k$  indicate the mass fraction, mole fraction, and molar concentrations of species  $k$  of  $M$ .
- The mean molecular mass is  $\overline{W}$  and the molar mass of species  $k$  is  $W_k$ .
- $T$  indicates temperature,  $p$  pressure,  $\rho$  density, and  $v = 1/\rho$  the specific volume, respectively.
- The enthalpy and internal energy per unit mass are  $h$  and  $u$ .

The following relations hold

$$x_k = \frac{\overline{W}}{W_k} y_k \quad (129)$$

$$c_k = \frac{\rho}{W_k} y_k \quad (130)$$

$$c_k = \frac{\rho}{\overline{W}} x_k \quad (131)$$

$$\overline{W} = \sum_{k=1}^M W_k x_k = \left( \sum_{k=1}^M y_k / W_k \right)^{-1} \quad (132)$$

# Reactions in a closed system



Consider a closed system for which the total mass  $M$  is conserved:

$$M = \sum_{k=1}^M M_k = \text{const} \quad (133)$$

where  $M_k = V\rho_k = V\rho y_k = My_k$  is the mass of species  $k$  with the system volume indicated by  $V$ , **not necessarily constant**.

Then the rate of change of  $M_k$  is written as:

$$\frac{dM_k}{dt} = M \frac{dy_k}{dt} = V \dot{\omega}_k W_k \quad (134)$$

$$\boxed{\frac{dy_k}{dt} = \frac{V}{M} \dot{\omega}_k W_k = \frac{W_k}{\rho} \dot{\omega}_k = v W_k \dot{\omega}_k} \quad (135)$$

In the equations above  $\dot{\omega}_k$  is the molar production rate of the  $k$  species by reaction ( $\text{mol cm}^{-3} \text{ s}^{-1}$ ). Note that Eq. (135) hold regardless of the details of the process.

# Rate of change of $c_k$



Based on Eqs. (129), (130), and (135), we may derive equations for the rate of change of molar concentrations  $dc_k/dt$ . Starting with the definition of  $c_k$ :

$$\frac{dc_k}{dt} = \frac{1}{W_k} \frac{d\rho y_k}{dt} = \frac{\rho}{W_k} \frac{dy_k}{dt} + \frac{y_k}{W_k} \frac{d\rho}{dt} = \dot{\omega}_k + \frac{\rho}{W_k} y_k \frac{1}{\rho} \frac{d\rho}{dt} = \dot{\omega}_k + c_k \frac{1}{\rho} \frac{d\rho}{dt}. \quad (136)$$

Since  $(d\rho/dt)/\rho = -(dv/dt)/v$ , one may write the equation above as

$$\boxed{\frac{dc_k}{dt} = \dot{\omega}_k - c_k \frac{1}{v} \frac{dv}{dt}} \quad (137)$$

- The rate of change of molar concentrations is due to reactions (first term) and changes in volume (second term).
- If  $V = \text{const}$  (equivalent to  $v = 0$ ), then the second term is zero and the rate of change of molar concentrations is due to reactions only ( $\dot{\omega}_k$ ).



# Rate of change of $x_k$

Start with taking the time derivative of Eq. (129):

$$\frac{dx_k}{dt} = \frac{1}{W_k} \frac{dy_k \bar{W}}{dt} = \frac{d}{dt} \left( \frac{y_k / (1/\bar{W})}{W_k} \right) = \frac{\bar{W}}{W_k} \frac{dy_k}{dt} - \frac{1}{(1/\bar{W})^2} \frac{y_k}{W_k} \frac{d(1/\bar{W})}{dt}. \quad (138)$$

We may write

$$\frac{d}{dt} \left( \frac{1}{\bar{W}} \right) = \sum_{j=1}^M \frac{dy_j/dt}{W_j} = \frac{1}{\rho} \sum_{j=1}^M \dot{\omega}_j, \quad (139)$$

so that Eq. (138) becomes

$$\frac{dx_k}{dt} = \frac{\bar{W}}{W_k} \frac{dy_k}{dt} - \frac{\bar{W} y_k}{W_k} \frac{\bar{W}}{\rho} \sum_{j=1}^M \dot{\omega}_j = \frac{\bar{W}}{\rho} \dot{\omega}_k - x_k \frac{\bar{W}}{\rho} \sum_{j=1}^M \dot{\omega}_j \quad (140)$$

$$\frac{dx_k}{dt} = \frac{\mathcal{R} T}{p} \left( \dot{\omega}_k - x_k \sum_{j=1}^M \dot{\omega}_j \right)$$

(141)

This equation shows that in the absence of chemical reaction, the mole fractions remain constant, which is expected.

# Adiabatic and constant pressure reaction I



We consider an adiabatic, constant mass system, which undergoes reactions at constant pressure. Describe the mixture composition by mass fractions.

Start with the definition of enthalpy and take a derivative with respect to time

$$h = \sum_{i=1}^M h_i(T) y_i = \text{const} \quad (142)$$

$$0 = \frac{dh}{dt} = \sum_{i=1}^M \frac{dh_i}{dT} y_i \frac{dT}{dt} + \sum_{i=1}^M h_i(T) \frac{dy_i}{dt} \quad (143)$$

$$0 = \sum_{i=1}^M C_{p,i} y_i \frac{dT}{dt} + \sum_{i=1}^M h_i(T) \frac{dy_i}{dt} \quad (144)$$

$$0 = C_p \frac{dT}{dt} + \sum_{i=1}^M h_i(T) \frac{dy_i}{dt} = C_p \frac{dT}{dt} + \sum_{i=1}^M h_i(T) \frac{W_i \dot{\omega}_i}{\rho} \quad (145)$$

# Adiabatic and constant pressure reaction II



The resulting system of equations is

$$\frac{dy_k}{dt} = \frac{W_k}{\rho} \dot{\omega}_k \quad (146)$$

$$\frac{dT}{dt} = -\frac{1}{\rho C_p} \sum_{i=1}^M h_i(T) W_i \dot{\omega}_i \quad (147)$$

$$\frac{dp}{dt} = 0 \quad (148)$$

which constitutes an “autonomous” system of nonlinear ODEs as it does not explicitly include a dependency on time  $t$ , but only on state  $(T, p, \mathbf{y})$ .

# Adiabatic and constant volume reaction I



We consider an adiabatic, constant mass system, which undergoes reactions at constant volume (or “specific volume”) Describe the mixture composition by mass fractions.

The derivation proceeds as before, letting  $u = \sum_{i=1}^M u_i(T) y_i = const$ :

$$\frac{du}{dt} = C_v \frac{dT}{dt} + \sum_{i=1}^M u_i(T) \frac{W_i \dot{\omega}_i}{\rho} = 0. \quad (149)$$

# Adiabatic and constant volume reaction II



$$\frac{dy_k}{dt} = \frac{W_k}{\rho} \dot{\omega}_k \quad (150)$$

$$\frac{dT}{dt} = -\frac{1}{\rho C_v} \sum_{i=1}^M u_i(T) W_i \dot{\omega}_i \quad (151)$$

$$\frac{1}{p} \frac{dp}{dt} = \frac{1}{T} \frac{dT}{dt} + \left( \sum_{i=1}^M \frac{dy_i/dt}{W_i} \right) \left( \sum_{i=1}^M \frac{y_i}{W_i} \right)^{-1}. \quad (152)$$

# Introduction to Jacobians



Jacobians are a fundamental concept in ordinary differential equations. In the case of zero-dimensional reactors, they are key to a successful time integration strategy.

Consider an autonomous system of non-linear ODEs  $d\mathbf{y}/dx = \mathbf{f}(\mathbf{y})$ , where  $\mathbf{y} \in \mathcal{R}^N$  and  $\mathbf{f} : \mathcal{R}^N \rightarrow \mathcal{R}^N$ .

Then the “Jacobian” of the system is a  $N \times N$  matrix:

$$\mathbf{J}(\mathbf{y}) = \frac{\partial \mathbf{f}}{\partial \mathbf{y}} \quad \text{or} \quad [\mathbf{J}]_{ij} = \frac{\partial f_i}{\partial y_j}. \quad (153)$$

Note that the Jacobian of a non-linear system of equation is not constant, rather changes with the solution vector  $\mathbf{y}$ .

Often, we shall look at the eigenvalues of  $\mathbf{J}$  and shall denote with  $\sigma(J) = \{\lambda_1, \dots, \lambda_N\}$  the “spectrum” of the Jacobian.

# The breakdown of the Jacobian for zero-d reactors

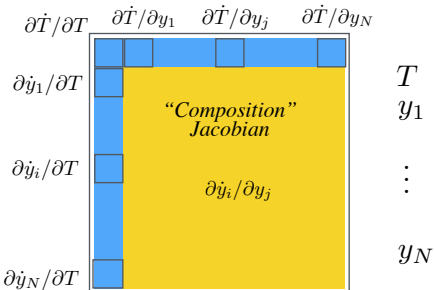


Recall the system of ODEs for an adiabatic, constant pressure, zero-dimensional reactor.

$$\frac{dT}{dt} = -\frac{1}{\rho C_p} \sum_{i=1}^M h_i(T) W_i \dot{\omega}_i$$

$$\frac{dy_k}{dt} = \frac{W_k}{\rho} \dot{\omega}_k = \dot{\Omega}_k$$

$$\frac{dp}{dt} = 0$$



It is clear that the system's Jacobian comprises a “composition Jacobian” block (yellow) and two vectors (blue) due to the dependence of  $\dot{T}$  on composition and the dependence of reactions, i.e.,  $\dot{y}_i$ , on temperature.

*Note that in the case of adiabatic/isochoric reactors ( $U = \text{const}$ ), pressure varies in time and the additional ODE for  $p(t)$  gives rise to a larger Jacobian*

# The concentration Jacobian is sparse

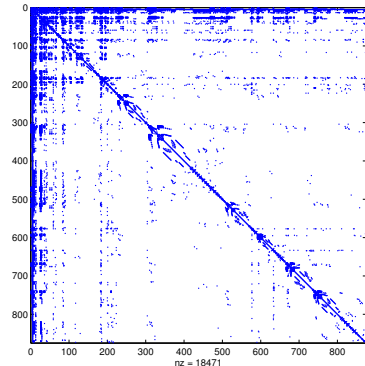


The concentration Jacobian,  $\partial \dot{\omega}_i / \partial c_j$  is a “sparse” matrix due to the loose chemical coupling between species.

A sparse matrix is a matrix in which most of the elements are zero. By contrast, if most of the elements are nonzero, the matrix is called dense.

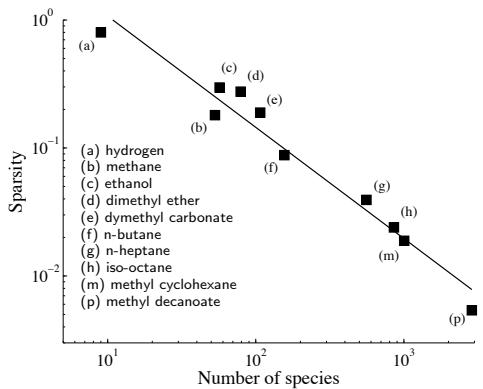
The “sparsity” of a matrix is the ratio of nonzero to the total number of elements.

*It is of paramount importance to exploit the underlying sparsity of the Jacobian matrix for the purpose of improving the computational performance of kinetics computations.*



Sparsity pattern for the 874 species iso-octane mechanism from LLNL. The sparsity is 2.42% ( $18471/874^2$ ).

# Sparsity in $\partial \dot{\omega}_i / \partial c_j$ across mechanisms



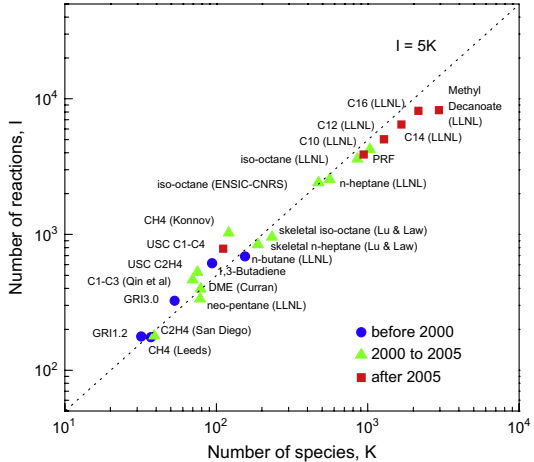
The sparsity of a wide selection of mechanisms has been assessed and shown in the figure to the left.

It is clear that, the larger then kinetics mechanism, i.e. the more species, the greater the sparsity.

See F. Bisetti, *Combust Theory Model* 16 (2011): 387-418 for more in-depth discussion.

- (a) hydrogen (Mueller et al., 1999); (b) methane (Smith et al., 1999); (c) ethanol (Marinov, 1999); (d) dimethyl ether (Kaiser et al., 2000); (e) dimethyl carbonate (Glaude et al., 2005); (f) *n*-butane (Marinov et al., 1998); (g) *n*-heptane (Curran et al., 2002); (h) iso-octane (Curran et al., 1998); (m) methyl cyclohexane (Pitz et al., 2007); (p) methyl decanoate (Herbinet et al., 2008).

# Trends in combustion mechanism size



There is a need to describe the combustion of “real” fuels (high number of carbon atoms)

Shown on the left is a plot from Lu and Law (PECS, 2009) showing that the size of mechanisms (measured as number of species  $K$  and number of reactions  $I$ ) is increasing steadily in time.

*This has real implications on computational costs of using those mechanisms.*

Adapted from Lu and Law, PECS 2009.

# Implications for Jacobian evaluation

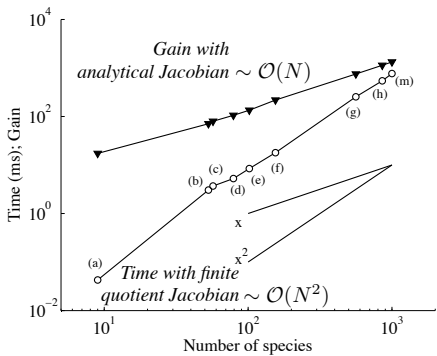


As part of implicit (stiff) integrators, Jacobians are evaluated hundreds of times.

## Finite quotient

$$\frac{\partial f_i}{\partial x_j} = \frac{f_i(\mathbf{x}_0 + \mathbf{e}_j \epsilon_j) - f_i(\mathbf{x}_0)}{\epsilon_j}$$

Costs scale as  $\mathcal{O}(N^2)$  as each rhs evaluation costs  $\mathcal{O}(N)$  and each evaluation is repeated  $N$  times. It also ignores sparsity.



## Analytical Jacobian

Costs scale as  $\mathcal{O}(N)$  for a single Jacobian evaluation and sparsity is exploited to avoid computing zero entries.

# The mass fractions Jacobian



- Mass fractions offer a natural description of the mixture's composition for reactions occurring at constant pressure and adiabatic conditions (no heat loss).

$$B_{ij} = \frac{\partial \dot{\Omega}_i}{\partial y_j} \quad (154)$$

where recall that  $\dot{\Omega}_i = \dot{W}_i \dot{\omega}_i / \rho$ .

- *Unfortunately, the mass fraction Jacobian  $\partial \dot{y}_i / \partial y_j$  is a **dense** matrix, i.e. all of its elements are nonzero!*
- One may derive an expression for the mass fraction Jacobian matrix that exposes some important simplifications
- The derivation is in Bisetti in Combustion Theory Model 16 (2011): 387-418.

# Decomposition of the Jacobian



The following decomposition applies

$$\begin{matrix} \text{DENSE} \\ \text{mass fractions} \\ \text{Jacobian} \end{matrix} = \begin{matrix} \text{SPARSE} \\ \text{concentrations} \\ \text{Jacobian} \end{matrix} + \begin{matrix} \text{Rank one} \\ \text{tensor} \end{matrix} + \begin{matrix} \text{Rank one} \\ \text{tensor} \end{matrix}$$

$\partial\dot{\Omega}_i/\partial y_j$        $\partial W_i\dot{\omega}_i/\partial W_j c_j$        $W_i p_i/W_j$        $\overline{W}\dot{\Omega}_i/W_j$

$$\frac{\partial\dot{\Omega}_i}{\partial y_j} = \frac{W_i}{W_j} \frac{\partial\dot{\omega}_i}{\partial c_j} - \frac{W_i}{W_j} p_i + \frac{\overline{W}}{W_j} \dot{\Omega}_i.$$

- The first is a rescaled concentration Jacobian (sparse):  $\partial\dot{\omega}_i/\partial c_j$ .
- The second  $W_i p_i/W_j$  and third  $\overline{W}\dot{\Omega}_i/W_j$  terms are full rank-one matrices

*The “dense” nature of the Jacobian  $\partial\dot{\Omega}_i/\partial y_j$  is due to rank-one matrices, not to the chemical kinetics mechanism. This can be exploited in iterative methods for non-linear systems (e.g., Krylov-based).*

# Chemical kinetics mechanisms are “stiff”



The initial value boundary problems arising from the ODE systems describing zero-dimensional reactors exhibit “stiffness”.

## But what is stiffness? And why should we care?

Quoting from “Solving ordinary differential equation II” by E. Hairer and G. Wanner:

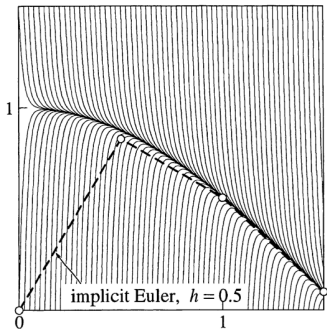
*The most pragmatic opinion is also historically the first one (Curtiss & Hirschfelder 1962): “stiff equations are equations where certain implicit methods, in particular BDF [Backward Differentiation Formulas] perform better, usually tremendously better, than explicit ones”.*

# An example of “stiff behavior” I

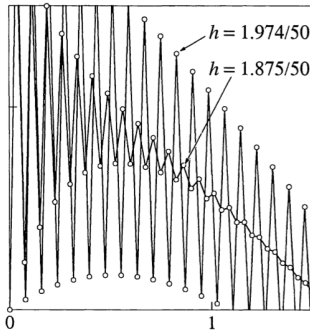


Curtiss & Hirschfelder (1952) explain stiffness on one-dimensional examples such as:

$$y' = -50(y - \cos x) \quad (155)$$



Solution curves with implicit Euler solution.

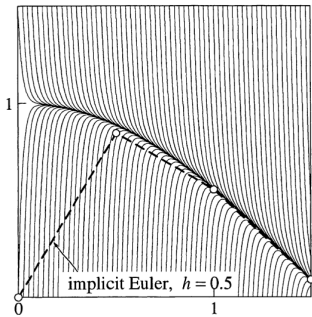


Explicit Euler for  $y(0) = 0$ ,  $h = 1.974/50$  and  $1.875/50$ .

# An example of “stiff behavior” II



- There is apparently a smooth solution in the vicinity of  $y \approx \cos x$ .
- All other solutions reach this one after a rapid “transient phase”.
- Such transients are typical of stiff equations, but are neither sufficient nor necessary.
- For example, the solution with initial value  $y(0) = 1$  (more precisely 2500/2501) has no transient.

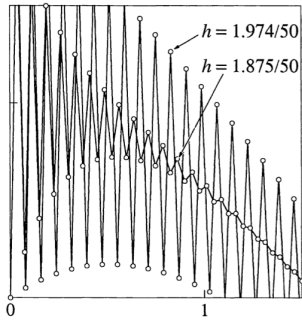


Solution curves with implicit Euler solution.

# An example of “stiff behavior” III



- The figure shows explicit Euler solutions for the initial value  $y(0) = 0$  and step sizes  $h = 1.974/50$  (38 steps) and  $h = 1.875/50$  (40 steps).
- Whenever the step size is a little too large (larger than  $2/50$ ), the numerical solution goes too far beyond the equilibrium and violent oscillations occur.



Explicit Euler for  $y(0) = 0$ ,  
 $h = 1.974/50$  and  $1.875/50$ .

# An example of “stiff behavior” IV

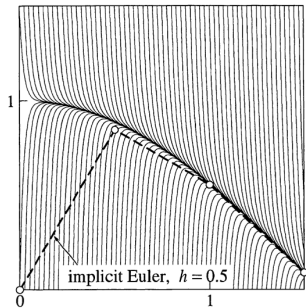


Looking for better methods for stiff differential equations, Curtiss and Hirschfelder (1952) discovered the BDF method, which is the “workhorse” numerical method in chemical kinetics.

The implicit Euler method:

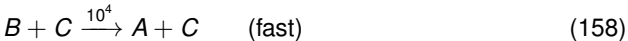
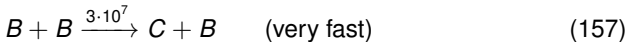
$$\frac{y_{n+1} - y_n}{h} = f(x_{n+1}, y_{n+1})$$

The dotted line consists of three implicit Euler steps and demonstrates impressively the good stability property of the implicit Euler method.



# Another example of “stiff behavior” I

This below is the well-known Robertson's kinetic system:



which leads to the equations:

$$A : y'_1 = -0.04y_1 + 10^4 y_2 y_3 \quad (159) \qquad y_1(0) = 1 \quad (162)$$

$$B : y'_2 = 0.04y_1 - 10^4 y_2 y_3 - 3 \cdot 10^7 y_2^2 \quad (160) \qquad y_2(0) = 0 \quad (163)$$

$$C : y'_3 = 3 \cdot 10^7 y_2^2 \quad (161) \qquad y_3(0) = 0 \quad (164)$$

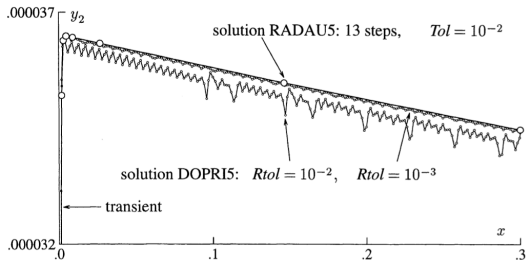
*The Robertson's example is often invoked as “sample kinetic mechanism”. Note it lacks the exponential dependence on temperature in real systems and non-linearities are limited to products.*



# Another example of “stiff behavior” II



Now, let us integrate the system with DOPRI5 (**explicit** Runge-Kutta) and with RADAU5 (**implicit** Runge-Kutta)



The solution  $y_2$  rapidly reaches a quasi-stationary position in the vicinity of  $y'_2 = 0$ , which in the beginning ( $y_1 = 1, y_3 = 0$ ) is at  $0.04 \approx 3 \cdot 10^7 y_2^2$ , hence  $y_2 \approx 3.65 \cdot 10^{-5}$ , and then very slowly goes back to zero again.

# Another example of “stiff behavior” III



The numerical solutions on the previous slide are obtained with DOPRI5 (explicit) for  $y_2$  with  $Rtol = 10^{-2}$  (DOPRI5: 209 steps),  $Rtol = 10^{-3}$  (DOPRI5: 205 steps) and  $Atol = 10^{-6} \times Rtol$ .

Conversely, the implicit integrator (RADAU5), takes only 13 steps.

- The explicit integrator (DOPRI) integrates the smooth solution by thousands of apparently unnecessary steps.
- The chosen step sizes are more or less independent of the chosen tolerance and seem to be governed by stability rather than by precision requirements.

**Conversely, an implicit Runge-Kutta code (such as RADAU5) integrates the equation without any problem!**

# Brief review of stability analysis I



The first analysis of instability phenomena and step size restrictions for hyperbolic equations was made in the famous paper of Courant, Friedrichs & Lewy (1928).

Let  $\varphi(x)$  be a smooth solution of  $y' = f(x, y)$ . We linearize  $f$  around  $(x, \varphi(x))$  as follows:

$$y'(x) = f(x, \varphi(x)) + \frac{\partial f}{\partial y}(x, \varphi(x))(y(x) - \varphi(x)) + \dots . \quad (165)$$

and introduce the “delta”  $\bar{y}(x) = y(x) - \varphi(x)$  to obtain

$$\bar{y}'(x) = f(x, \varphi(x)) \cdot \bar{y}(x) + \dots = J(x)\bar{y}(x) \quad (166)$$

As a first approximation, we consider the Jacobian  $J(x)$  as constant and neglect the error terms. Omitting the bars we arrive at the system of linear ODEs

$$y' = Jy \quad (167)$$

# Brief review of stability analysis II



If we now apply Euler's method and set  $R(hJ) = 1 + hJ$ , we obtain:

$$y_{m+1} = y_m + hJy_m = R(hJ)y_m \quad (168)$$

The behavior of this equation is studied by transforming  $J$  to Jordan canonical form. We suppose that  $J$  is diagonalizable with eigenvectors  $v_1, \dots, v_n$  and write  $y_0$  in this basis as

$$y_0 = \sum_{i=1}^n \alpha_i v_i \quad (169)$$

Then

$$y_m = \sum_{i=1}^n (R(h\lambda_i))^m \alpha_i v_i \quad (170)$$

where the  $\lambda_i$  are the corresponding eigenvalues.

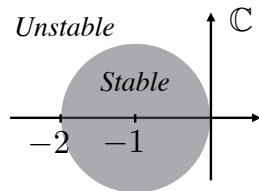
# Brief review of stability analysis III



Clearly  $y_m$  remains bounded for  $m \rightarrow \infty$  (i.e., an infinite number of steps), if, for all eigenvalues  $\lambda_i$ , the complex number  $z = h\lambda_i$  lies in the set:

$$\begin{aligned} S &= \{z \in \mathbb{C}; |R(z)| \leq 1\} \\ &= \{z \in \mathbb{C}; |z - (-1)| \leq 1\} \end{aligned} \quad (171)$$

which is the circle of radius 1 and center -1.



This explains the issues encountered in solving of  $y' = -50(y - \cos x)$ . There we have  $\lambda = -50$ , and  $h\lambda \in S$  implies that it must be  $0 \leq h \leq 2/50$ , in perfect accordance with the numerical observations.

The stability condition above impose strict restrictions on the size of  $h$  for stable time steps with Euler forward if the eigenvalues  $\lambda_i$  are very large, e.g.,  $|\operatorname{Re}[\lambda_i]| \gg 1$ .

# Integrating kinetics -Stability Analysis for Explicit Runge-Kutta Methods-

The family of explicit Runge-Kutta methods is an example of high-order explicit methods.

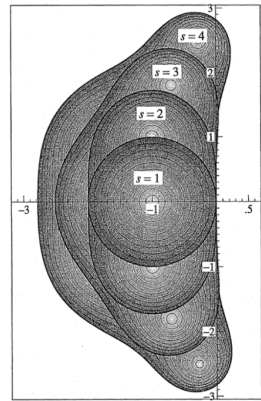
Using the Dahlquist test equation

$$y' = \lambda y, \quad y_0 = 1, \quad z = h\lambda, \quad (172)$$

one may show that if the Runge-Kutta method is of order  $p$ , then its “stability function”  $R(z)$  is

$$R(z) = 1 + z + \frac{z^2}{2!} + \dots + \frac{z^p}{p!} + \mathcal{O}(z^{p+1}) \quad (173)$$

and all explicit R-K methods with a number of stages  $s = p$  have the domains of stability on the right.



Stability domains for explicit Runge-Kutta methods of order  $p = s$ .

# Stability of the implicit Euler's method



Now consider the implicit Euler's method (also known as Euler backward):

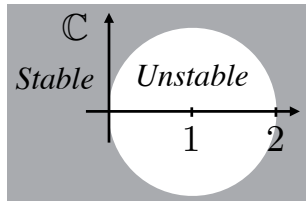
$$y_1 = y_0 + hf(x_1, y_1) \quad (174)$$

and apply it to Dahlquist's equation to obtain

$$y_1 = y_0 + h\lambda y_1 \quad (175)$$

After solving for  $y_1$  we have:

$$y_1 = R(h\lambda)y_0 \quad \text{with} \quad R(z) = \frac{1}{1 - z} \quad (176)$$



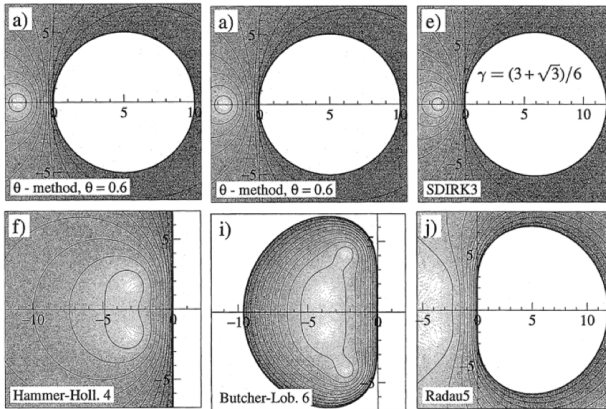
The stability domain is the exterior of the circle with radius 1 and centre 1.

*The stability domain thus covers the entire negative half-plane and a large part of the positive half-plane as well. The implicit Euler method is **very stable**.*

# Stability of implicit methods



It turns out that such extended stability regions are typical of many implicit methods (see Hairer and Wanner for details) as shown below for various implicit Runge-Kutta methods.



# Backward Differentiation Formulas I



Backward Differentiation Formulas (or BDF) are widely used *multistep formulas* for “stiff” differential equations (Gear 1971, Curtiss and Hirschfelder, 1952).

In the combustion kinetics community, they are at the basis of many “workhorse” codes, such as CVODE (or DVODE, DASSL, etc.)

Assume that the approximations  $y_{n-k+1}, \dots, y_n$  to the exact solution of  $y' = f(x, y)$   $y(x_0) = y_0$  are known.

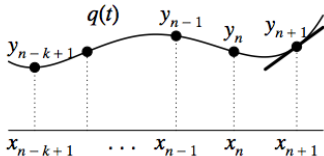
In order to derive a formula for  $y_{n+1}$  we consider the polynomial  $q(x)$  which interpolates the values  $\{(x_i, y_i) | i = n - k + 1, \dots, n + 1\}$ .

Note that for implicit formulas (the “useful” BDF), one imposes that the polynomial  $q(x)$  satisfies the differential equation at  $(x_{n+1}, y_{n+1})$

$$q'(x_{n+1}) = f(x_{n+1}, y_{n+1}) \quad (177)$$

# Backward Differentiation Formulas II

The BDF with  $q'(x_{n+1}) = f(x_{n+1}, y_{n+1})$  are shown below



After manipulating the definition of the backward differences formulas, one obtains

$$\sum_{j=1}^k \frac{1}{j} \nabla^j y_{n+1} = h f_{n+1} = h f(x_{n+1}, y_{n+1}) \quad (178)$$

where the backward differences are

$$\nabla^{j+1} f_n = \nabla^j f_n - \nabla^j f_{n-1} \quad \text{with} \quad \nabla^0 f_n = f_n. \quad (179)$$

For example, for  $k = 1$ , one obtains Euler backward (implicit Euler).

# Backward Differentiation Formulas III

The collection of (implicit) BDF formulas are ( $1 \leq k \leq 5$ ):

$$k = 1 \quad y_{n+1} - y_n = hf_{n+1} \quad (180)$$

$$k = 2 \quad \frac{3}{2}y_{n+1} - 2y_n + \frac{1}{2}y_{n-1} = hf_{n+1} \quad (181)$$

$$k = 3 \quad \frac{11}{6}y_{n+1} - 3y_n + \frac{3}{2}y_{n-1} - \frac{1}{3}y_{n-2} = hf_{n+1} \quad (182)$$

$$k = 4 \quad \frac{25}{12}y_{n+1} - 4y_n + 3y_{n-1} - \frac{4}{3}y_{n-2} + \frac{1}{4}y_{n-3} = hf_{n+1} \quad (183)$$

$$k = 5 \quad \frac{137}{60}y_{n+1} - 5y_n + 5y_{n-1} - \frac{10}{3}y_{n-2} + \frac{5}{4}y_{n-3} - \frac{1}{5}y_{n-4} = hf_{n+1} \quad (184)$$

For  $k > 6$  the BDF-methods are unstable.

The integrator CVODE adopts a “variable” order and “variable step size” approach, whereby the order of the BDF (typically between 2 and 5) and the step size vary to meet user-defined error tolerances.



# CVODE & SUNDIALS



The software suite “SUNDIALS” (SUite of Nonlinear and DIfferential/ALgebraic equation Solvers) provides robust time integrators and nonlinear solvers that can easily be incorporated into existing simulation codes.

It is actively developed and maintained by a team of applied mathematicians and software developers at LLNL (Carol S. Woodward, Daniel R. Reynolds, Alan C. Hindmarsh, and Lawrence E. Banks).

CVODE is part of SUNDIALS and is a solver for initial value problems for ordinary differential equation (ODE) systems. When the “stiff” option is used, it implements variable order, variable step-size BDF methods.

More at <http://computation.llnl.gov/casc/sundials/main.html>

*Virtually all combustion codes that perform integration of kinetics problems rely on CVODE or one of its variants (e.g., DVODE)*

# Numerical tests



In what follows, we shall show some numerical tests performed for

- Methane/air reactive mixtures with GRIMech 3.0: **53 species and 324 reactions.**
- Hydrogen/air reactive mixtures with Mueller, Kim, Yetter, Dryer (Int J Chem Kin, 1999): **9 species and 21 reactions.**

All integrations are performed with Cantera (v2.1.2, gcc v4.6.3 with `-O3` flags) through its MATLAB interface and the MATLAB (R2014a) integrator `ode15s` (interface to CVODE).

Tests are performed on a workstation equipped with two 10 core Intel Xeon CPU E5-2680 v2 @ 2.80GHz processors and 256 GB memory

# The ignition of $\text{H}_2$ and $\text{CH}_4$ mixtures

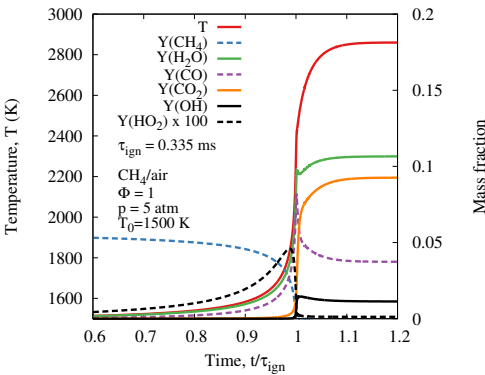


We consider the ignition of mixtures of fuel (hydrogen and methane) and air at given equivalence ratios  $\Phi$ , pressure  $p_0$  and initial temperature  $T_0$ .

In the examples that follow, the mixture enthalpy  $h$  and pressure  $p$  are constant.

The evolution of  $T$  and the mass fractions of selected species is shown for a stoichiometric ( $\Phi = 1$ ) methane/air mixture at 5 atm and  $T_0 = 1500$  K.

At those conditions, the ignition delay time is  $\tau_{\text{ign}} = 0.335$  ms.



# The spectra of H<sub>2</sub> and CH<sub>4</sub> during ignition I



Let  $T(t)$ ,  $\mathbf{Y}(t)$  and  $p(t)$  indicate the state of the mixture in time during the ignition of the fuel/air mixture.

- The equations describing the evolution of the mixture at constant enthalpy and pressure are solved for  $t \in [0, 1.5\tau_{ign}]$
- The Jacobian matrix  $[\mathbf{B}]_{ij} = \partial \dot{\Omega}_i / \partial y_j$  is assembled at every discrete time step and its spectrum computed

## Some general statements

- The eigenvalues of  $\mathbf{B}$  lie on or very close to the real axis (i.e.,  $Im\{\lambda\} \approx 0$ ). Most of them have  $Re\{\lambda\} < 0$  (dissipative modes), while a few have  $Re\{\lambda\} > 0$  (explosive modes).
- $\max\{|Re[\lambda^-]|\} \gg \max\{|Re[\lambda^+]\|}$ , where  $\lambda^-$  belongs to the set s.t.  $Re[\lambda] < 0$  and  $\lambda^+$  belongs to the set s.t.  $Re[\lambda] > 0$ .

# The spectra of H<sub>2</sub> and CH<sub>4</sub> during ignition II



In considering the spectrum of the Jacobian  $\sigma(\mathbf{B})$ , there are two quantities to focus our attention on:

- The “largest” eigenvalue with negative real part

$$\lambda_{\max} = \max\{|Re[\lambda^-]|\} \quad \text{with} \quad \lambda^- \text{ s.t. } Re\{\lambda\} < 0 \quad (185)$$

*The magnitude of  $\lambda_{\max}$  governs the largest stable step size  $h$  that can be taken with an explicit method.*

- The value of the product of  $\lambda_{\max}$  and the ignition delay time  $\tau_{ign}$ , taken to represent the desired integration interval:

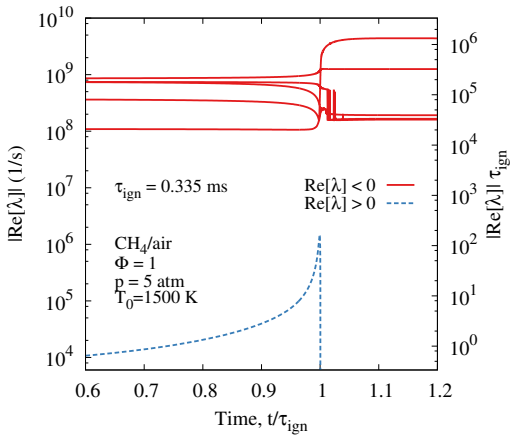
$$N_{steps} = \lambda_{\max} \tau_{ign} \quad (186)$$

*The quantity  $\lambda_{\max} \tau_{ign}$  represents an order-of-magnitude estimate of how many “explicit” time steps are required to integrate the equations until ignition.*

# The spectrum of methane/air ignition



We consider the ignition of methane/air ( $\Phi = 1$ ) at 5 atm, from 1500 K. The real part of selected  $\lambda^+$  and  $\lambda^-$  eigenvalues is shown in the figure

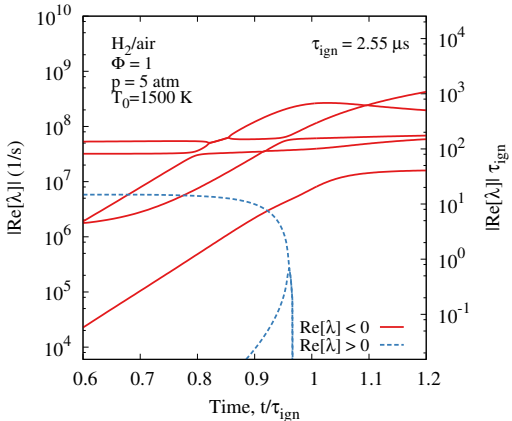


Methane/air ignition displays time scales faster than 1 ns ( $10^{-9} \text{ s}$ ), including the pre-ignition phase, making explicit methods impractical

After ignition, the smallest time scale becomes even smaller

Note the rise of the positive eigenvalue in correspondence of ignition

# The spectrum of hydrogen/air ignition



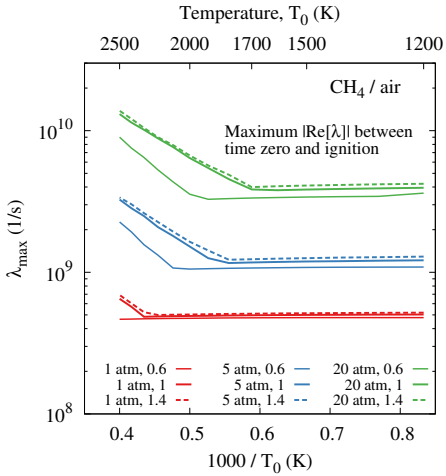
We consider the ignition of hydrogen/air ( $\Phi = 1$ ) at 5 atm, from 1500 K.

Hydrogen/air ignition displays time scales faster than 10 ns ( $10^{-8} \text{ s}$ ), but somewhat less fast than methane.

When normalized by the ignition time, though,  $\lambda_{\max}^- \tau_{ign} \leq 10^3$ , which is much more favorable than for methane.

*In the case of hydrogen/air, the problem is less “stiff” than for methane/air ignition because the integration interval or “large” time scale (i.e.,  $\tau_{ign}$ ) is significantly shorter than for methane, leading to a smaller scale gap.*

# The dependence of $\lambda_{\max}$ on $\phi$ , $p_0$ , and $T_0$ for methane/air



Pressure has a very important effect on the smallest time scale of the reactive system, which **decreases as pressure increases**, e.g., from 2 ns (1 atm) to 0.25 ns (20 atm).

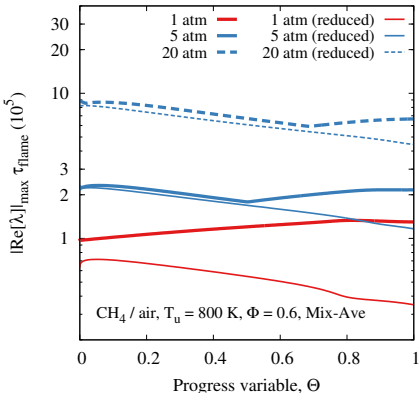
Equivalence ratio has hardly any effect.

The effect of the initial temperature is negligible for low temperatures, but becomes important for very large  $T_0$  (e.g.,  $T_0 \geq 1700$  K), when  $\lambda_{\max}^- \uparrow$  with  $T_0 \uparrow$ .

# The spectrum in premixed methane/air flames



We compute  $\lambda_{\max}^-$  based on the mixture state across a premixed laminar methane/air flame.



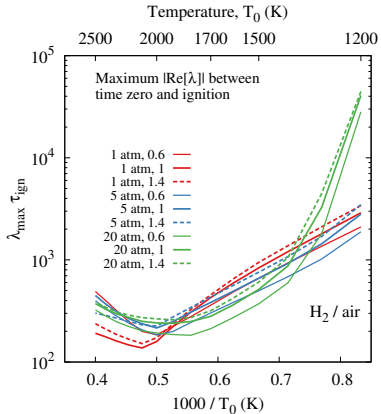
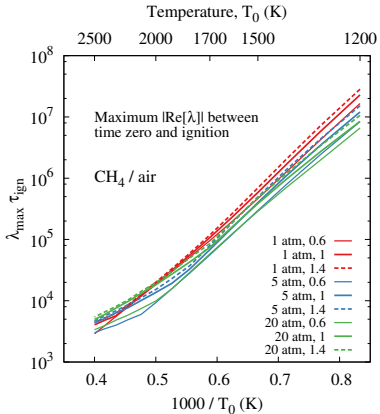
The largest eigenvalue is normalized by the “flame time”

$\tau_{\text{flame}} = \delta_T / s_L$ : time taken for the flame to propagate over a distance equal to its thermal thickness.

Calculations are repeated at various pressures (1, 5, and 20 atm) and with two mechanisms (GRIMech 3.0 and a 16 species reduced one)

*The number of time steps required to advance a  $\text{CH}_4/\text{air}$  flame with an explicit method by one flame thickness ( $\delta_T$ ) is  $\mathcal{O}(10^5 - 10^6)$ , increasing with pressure.*

# Normalized scales: $\lambda_{\max}^- \tau_{ign}$

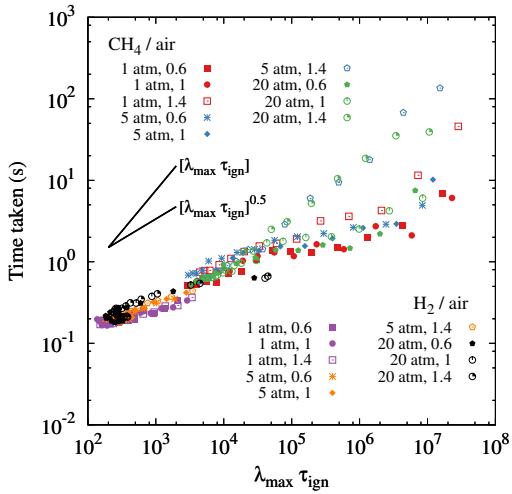


The quantity  $\lambda_{\max}^- \tau_{ign}$  increases rapidly for decreasing initial temperature  $T_0$  for methane (left), making the problem more “stiff”. The integration of hydrogen (right) is significantly less “stiff”, since  $\tau_{ign,H_2} \ll \tau_{ign,CH_4}$ .

# Wall-clock time for ignition



The wall-clock time taken for `ode15s` to integrate the reactive system over the time interval  $t \in [0, 1.5\tau_{ign}]$  is shown below



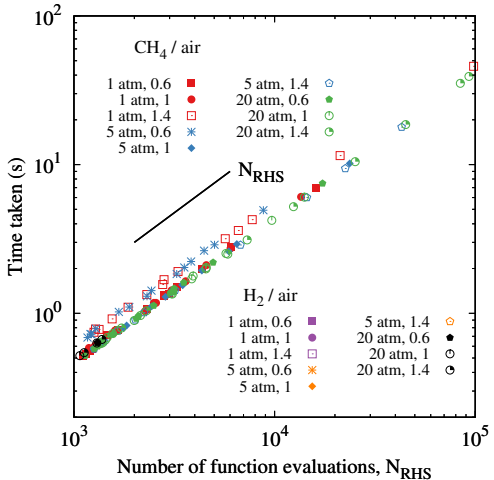
Integrating hydrogen is less demanding than integrating the methane mechanism

Regardless of the mechanism, the time taken scales as the square root of the time scale gap, i.e.

$$\text{Cost} \propto [\lambda_{\max}^{-} \tau_{ign}]^{1/2}$$

which is significantly better than an “explicit method scaling”  
 $\propto \lambda_{\max}^{-} \tau_{ign}.$

# RHS evaluations



For the cases at hand, the wall-clock time increases linearly with the number of evaluations of the rhs function of the ODE system.

The cost of integrating the methane/air and hydrogen/air systems is due mostly to the cost of evaluating the RHS

Thus, the overhead of solving nonlinear (and linear!) systems due to the implicit method are negligible.

*This behavior is typical of “small” combustion kinetic mechanisms with less than  $\mathcal{O}(100)$  species. Recall that GRIMech has 53 species and the hydrogen mechanism has 9 species.*

# Comparison of methane and iso-octane spectral properties

From hydrogen to methane, the “spectral gap” between the macro time scales of interest (i.e.  $\tau_{ign}$ ) and the fastest time scales ( $1/\lambda_{\max}$ ) widens.

*Do mechanisms larger than methane display an even wider gap? What about the spectral properties of very large mechanisms for “realistic” fuels, e.g., iso-octane*

We consider the ignition of a stoichiometric iso-octane/air mixture at 1500 K.

The iso-octane mechanism features 874 species and 3796 reactions (Curran et al., 1998).

In addition to  $|Re\{\lambda^-\}|_{\max}$  and  $|Re\{\lambda^+\}|_{\max}$ , we consider two measures of “non-normality” of the Jacobian matrix: (a) the “Henrici measure”  $\kappa_H$ :

$$\kappa_H(A) = ||A^H A - AA^H|| / ||A||_2^2$$

and (b) the condition number of the matrix of the eigenvectors  $\text{cond}(V)$ .

# Comparison of methane and iso-octane spectral properties



	methane	iso-octane
$ Re\{\lambda^-\} _{\max}$	$4.35 \times 10^8$	$5.44 \times 10^{14}$
$ Re\{\lambda^+\} _{\max}$	$6 \times 10^3$	$5 \times 10^4$
$\kappa_H$	0.815	0.926
cond( $V$ )	$10^4$	$3 \times 10^{22}$

Adapted from F. Bisetti, Combust Theory Model 16 (2011): 387-418.

- The iso-octane mechanism has significantly larger  $|Re\{\lambda^-\}|_{\max}$  compared to methane, indicating a much larger degree of “stiffness”.
- Both mechanisms give rise to highly non-normal Jacobians, with “non-normality” being more apparent for the iso-octane mechanism
- The iso-octane Jacobian is very ill-conditioned, indicating that the eigenvectors are very sensitive to perturbations in the Jacobian matrix



# Low mach number approach to the solution of the reactive N-S equations

# The low Mach nr approximation



If  $U \ll a$ , where  $U$  is a characteristic velocity and  $a$  is the speed of sound, the low Mach nr approximation applies (McMurtry et al. 1985, Sivashinsky 1979, Rehm and Baum 1978, Chu and Kovasznay 1957)

Take constant properties  $\mu$ ,  $\lambda$ ,  $\rho\mathcal{D}$ , and  $\gamma$ .

$$\frac{D\rho}{Dt} = \rho \nabla \cdot \mathbf{u} \quad (187)$$

$$\gamma Ma^2 \rho \frac{D\mathbf{u}}{Dt} = -\nabla p + \frac{\gamma Ma^2}{\mathfrak{R}} \nabla \cdot \tau \quad (188)$$

with reference quantities  $\tilde{U}$ ,  $\tilde{\rho}$ ,  $\tilde{T}$ ,  $\tilde{L}$ ,  $\tilde{p} = \tilde{\rho}R\tilde{T}$ , and  $\tilde{t} = \tilde{L}/\tilde{U}$  and expand the relevant variables in  $\varepsilon = \gamma Ma^2$  as follows

$$p(\mathbf{x}, t) = p^{(0)} + \varepsilon p^{(1)} + \varepsilon^2 p^{(2)} + \dots \quad (189)$$

$$\mathbf{u}(\mathbf{x}, t) = \mathbf{u}^{(0)} + \varepsilon \mathbf{u}^{(1)} + \varepsilon^2 \mathbf{u}^{(2)} + \dots \quad (190)$$

$$\rho^{(0)} = p^{(0)} RT^{(0)} \quad (191)$$

## ...continued



Substitute the expansion in the expression above and gather the zero-order terms in  $\varepsilon$

$$\frac{D\rho^{(0)}}{Dt} = \rho^{(0)} \nabla \cdot \mathbf{u}^{(0)} \quad (192)$$

$$\nabla p^{(0)} = 0 \quad (193)$$

and from the first-order momentum equation we recover an expression for the zero-order component of  $\mathbf{u}$

$$\rho^{(0)} \frac{D\mathbf{u}^{(0)}}{Dt} = -\nabla p^{(1)} + \frac{1}{\mathfrak{R}} \nabla \tau^{(0)} \quad (194)$$

An expression for  $\nabla \cdot \mathbf{u}^{(0)}$  from continuity provides insight into the approximation

$$\nabla \cdot \mathbf{u}^{(0)} = \frac{1}{\text{Pr} \mathfrak{R}} \nabla^2 T^{(0)} + \text{Da} \sum \frac{h_{0,i} \dot{\omega}_i}{T^{(0)}} \quad (195)$$

# Summary on Low Mach nr approximation



- In the limit  $U \ll a$ , split pressure as  $p(\mathbf{x}, t) = p^{(0)} + \gamma Ma^2 p^{(1)}$ , where  $p^{(0)}(t)$  is called the “thermodynamic pressure” and  $p^{(1)}(\mathbf{x}, t)$  is called the “hydrodynamic pressure”
- $\nabla \cdot \mathbf{u}^{(0)}$  is not negligible and related to heat release and conduction: acts as a kinematic constraint
- On the contrary,  $\nabla p^{(0)} = 0$  and for “open atmospheric flames”,  $p^{(0)} = \text{const.}$
- The momentum equation reads:

$$\rho \frac{D\mathbf{u}}{Dt} = -\nabla p^* + \nabla \cdot \mu \left( \nabla \mathbf{u} + \nabla \mathbf{u}^T - \frac{2}{3} (\nabla \cdot \mathbf{u}) \mathbf{I} \right) \quad (196)$$

- A variable coefficient Poisson equation is derived for  $p^*$ , much like in velocity-projection methods, but including heat release effects (see Tombooulides et al. 1997).

# Low Mach approximation



Worldwide, there exist several groups that adopt the low Mach number limit of the reactive Navier-Stokes equations.

## A partial list...

- Our group at King Abdullah University of Science and Technology
- In Germany (RWTH Aachen): H. Pitsch
- In the US: Prof. M. Mueller (Princeton), Prof. G. Blanquart (Caltech),  
Prof. V. Raman (U Michigan), Prof. M. Ihme (Stanford Univ),  
Prof. M. Smooke (Yale Univ), Dr. John Bell (LBNL)
- In France, Dr. V. Moureau (CORIA)
- In Switzerland, Profs. Frouzakis and Tomboulides (ETH)

# Spatial & temporal discretizations



*Spatial discretization* (see Desjardins et al. JCP 2008)

- Finite difference on Cartesian grid, staggered grids in space and time
- Second order central difference spatial discretization for convective and diffusive momentum terms
- WENO5 for spatial discretization of convective scalar fields

*Temporal discretization*

- Semi-implicit time integration via fractional step scheme with approximate-factorization (Kim & Moin 1985, Pierce & Moin 2005)
- Variable coefficients Poisson equation for the pressure  $p^*$  solved via Hypre's PCG with one iteration of PFMG (multi-grid) preconditioner
- Reactive scalars use a stiff predictor step (point-wise chemical reactions), but no corrector

# The semi-implicit time advancement



Let us consider a single ordinary differential equation:

$$\frac{du}{dt} = f(u), \quad (197)$$

where  $f(u)$  is non-linear and write

$$u_1 - u_0 = hf((u_1 + u_0)/2) \quad (198)$$

The time discretization above is known as the implicit midpoint rule (Hairer, Nørsett and Wanner 2008).

Solve with two Newton-Raphson iterations ( $u_1^{(0)} = u_0$  and  $p = 0, 1$ )

$$\left[ 1 - \frac{h}{2} \frac{\partial f}{\partial u} \right] (u_1^{(p+1)} - u_1^{(p)}) = u_0 - u_1^{(p)} + hf((u_0 + u_1^{(p)})/2) \quad (199)$$

The resulting scheme is A-stable, albeit not L-stable, Rosenbrock method (2-stage, 2-order) with  $\gamma = 1/2$ ,  $b_1 = 0$ ,  $b_2 = 1$ ,  $\alpha_{21} = 1/2$ , and  $\gamma_{21} = -1/2$ .

# Application to N-S equations



---

## Algorithm 1 Time advancement for low Mach reactive N-S

---

- 1: **while**  $t < t_{\text{end}}$  **do**
  - 2:    $S_{\phi}^{\text{rxn}} \leftarrow \phi^* - \phi_0$  (point-wise implicit)
  - 3:    $u_1^{(0)} \leftarrow u_0, \phi_1^{(0)} \leftarrow \phi_0, \rho_1^{(0)} \leftarrow \rho_0$
  - 4:   **for**  $p = 0$  to  $1$  **do**
  - 5:      $\phi_1^{(p)} \rightarrow \phi_1^{(p+1)}$  (scalar advance)
  - 6:      $\rho_1^{(p+1)} \leftarrow \hat{\rho}(\phi_1^{(p+1)})$  (evaluate density)
  - 7:      $u_1^{(p)} \rightarrow \tilde{u}_1^{(p+1)}$  (velocity advance)
  - 8:      $p_1^{*(p)} \rightarrow p_1^{*(p+1)}$  (solve Poisson for pressure  $p^*$ )
  - 9:      $\tilde{u}_1^{(p+1)} \rightarrow u_1^{(p+1)}$  (correct velocity)
  - 10:     $t \leftarrow t + \Delta t$
-

# Scalar advancement



Let  $\phi = (T, Y_1, \dots, Y_M)$  indicate the vector of scalar variables,  $\phi_0$  the current value and  $\phi_1$  the value at  $t + t + \Delta t$ .

## Step 1.

Integrate at each grid-point the following IVP

$$\frac{\partial \phi}{\partial t} = f(\phi), \quad (200)$$

$$\phi(t=0) = \phi_0 \quad (201)$$

and let

$$S_\phi^{\text{rxn}} = \frac{1}{\Delta t} (\phi^* - \phi_0) \quad (202)$$

where  $\phi^*$  is the result from the IVP above.

The integration is performed with CVODE/SUNDIALS, analytical Jacobian, and optimized rate expression.

# Scalar advancement



## Step 2.

Now advance the scalars globally due to transport (diffusion & convection) and (frozen) reaction

$$\left[1 - \frac{\Delta t}{2} \left[ \frac{\partial H^d}{\partial \phi} \right] \right] (\phi_1^{(p+1)} - \phi_1^{(p)}) = \frac{\rho_0}{\rho_1^{(p)}} \phi_0 - \phi_1^{(p)} + \frac{\Delta t}{\rho_1^{(p)}} (H^{c+d} + S_\phi^{\text{rxn}}) \quad (203)$$

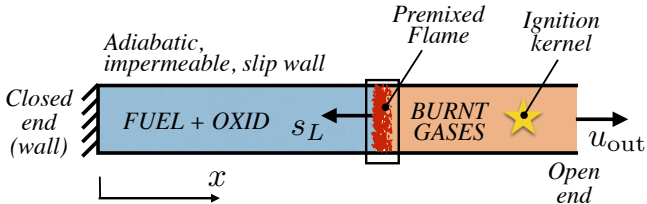
$$\begin{aligned} H &= H((\rho \mathbf{u})_1^{(p)}, (\phi_0 + \phi_1^{(p)})/2, (\rho \mathcal{D})_0) \\ &= -\nabla \cdot (\rho \mathbf{u} \phi) + \nabla \cdot (\rho \mathcal{D} \nabla \phi) \end{aligned} \quad (204)$$

- Convective fluxes  $H^c$  are treated explicitly, while diffusive ones  $H^d$  are semi-implicit
- Alternating Direction Implicit (ADI) for penta-diagonal system
- For simplicity, transport properties are “frozen” at time  $t$
- Note that momentum  $\rho \mathbf{u}$  is updated from  $p = 0$  to  $p = 1$

# Some numerical experiments



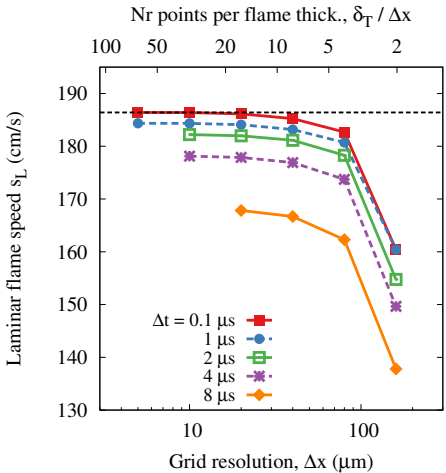
We consider the propagation of laminar, premixed methane/air flames at 1 atm, 800 K, and lean conditions ( $\Phi = 0.7$ ) in a “numerical flame tube”



The domain is one-dimensional and extends  $L = 2$  cm in length. Ignition occurs close to the “open end” and the flame propagates right to left towards the “end wall”.

The domain is discretized with a uniform mesh of cell size  $5 \leq \Delta x \leq 160 \mu\text{m}$  and the reactive N-S equations are integrated with a time step  $1 \leq \Delta t \leq 10 \mu\text{s}$ .

# Spatial convergence

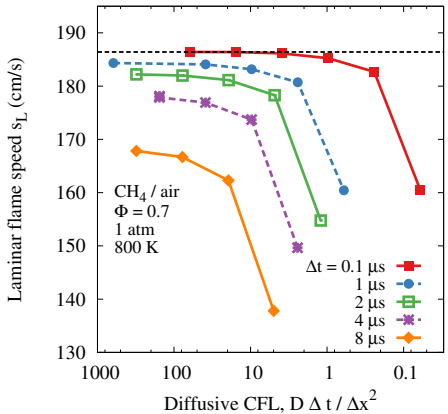


Convergence properties for the flame speed are shown for a premixed methane/air flame ( $\Phi = 0.7$ ,  $T_u = 800$  K, and  $p = 1$  atm).

About 10 points across the flame thickness ( $\delta_T$ ) are needed for convergence of the flame speed, regardless of the time step size.

Time step size of about  $1 \mu\text{s}$  appear adequate for resolving the flame speed

# Diffusive CFL in implicit time advancement



The semi-implicit time advancement for reactive scalars allows for remarkably large diffusive CFL, defined as

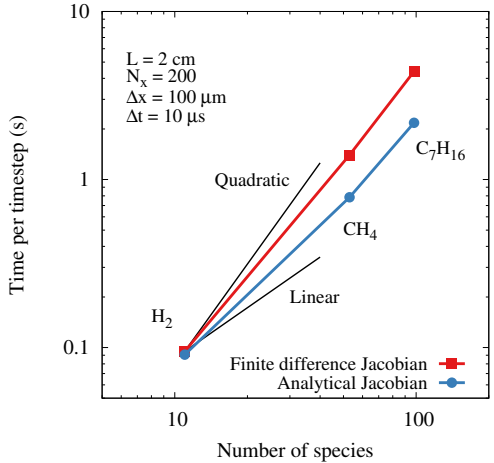
$$\text{CFL}_{\text{diff}} = \mathcal{D} \frac{\Delta t}{\Delta x^2}. \quad (205)$$

As  $\Delta x \rightarrow 0$  for a constant  $\Delta t$ , the CFL condition increases well beyond unity.

Stable calculations with diffusive CFL numbers in excess of 100 have been performed successfully with no difficulty

*The ability of converging the solution spatially at CFL numbers in excess of 100 is truly a distinct advantage of implicit time advancement.*

# Computational costs

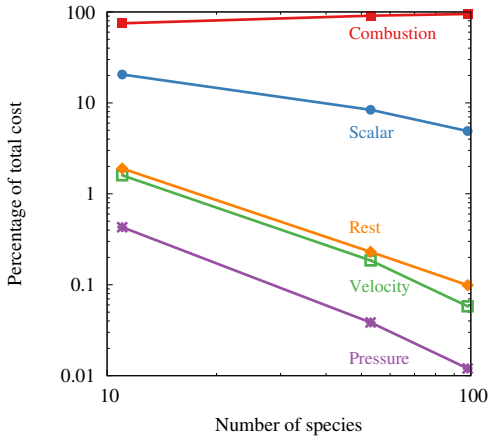


Flame propagation calculations are repeated for combustion models with increasing number of species: hydrogen (11), methane (53), and a reduced n-heptane mechanism (98).

The calculations are repeated with analytical and finite difference Jacobian, showing the former is preferable. In the case of n-heptane, simulations are twice as fast with the analytical Jacobian.

*The cost scales rather favorably, somewhere between linearly and quadratically with the number of species.*

# Costs' breakdown



The two most costly portions of the simulation are:

- The integration of the chemical kinetics (pointwise, within operator splitting)
- The semi-implicit time advancement of the reactive scalars due to transport

As the size of the mechanism increases, combustion kinetics dominates computational costs, reaching  $\approx 100\%$ .

*While in the case of three-dimensional simulations, the time advancement of scalar species plays a more important role, the integration of the chemical species source terms remains the most demanding step.*

# References I



- Bird, R. B., W. E. Stewart, and E. N. Lightfoot (2007). *Transport phenomena*. New York: John Wiley & Sons.
- Chapman, S. and T.G. Cowling (1991). *The mathematical theory of non-uniform gases*. 3rd ed. Cambridge University Press.
- Curran, H. J. et al. (1998). "A Comprehensive Modeling Study of n-Heptane Oxidation". In: *Combust. Flame* 114. Downloaded from [https://www-pls.llnl.gov/?url=science\\_and\\_technology-chemistry-combustion-iso\\_octane\\_version\\_3](https://www-pls.llnl.gov/?url=science_and_technology-chemistry-combustion-iso_octane_version_3). Website version LLNL-MI-421507. Review and release date: December 16, 2009, pp. 149–177.
- Curran, H. J., W. J. Pitz, and C. K. Westbrook (2002). UCRL-WEB-204236.
- Egolfopoulos, F N et al. (2014). "Advances and challenges in laminar flame experiments and implications for combustion chemistry". In: *Progress in Energy and Combustion Science* 43.C, pp. 36–67.

## References II



- Glaude, P. A., W. J. Pitz, and M. J. Thomson (2005). "Chemical kinetic modeling of dimethyl carbonate in an opposed-flow diffusion flame". In: *Proc. Combust. Inst.* 30.1, pp. 1111–1118.
- Herbinet, O., W. J. Pitz, and C. K. Westbrook (2008). "Detailed chemical kinetic oxidation mechanism for a biodiesel surrogate". In: *Combust. Flame* 154.3, pp. 507–528.
- Kaiser, E. W. et al. (2000). "Experimental and Modeling Study of Premixed Atmospheric-Pressure Dimethyl Ether- Air Flames". In: 104.35, pp. 8194–8206.
- Marinov, N. M. (1999). "A detailed chemical kinetic model for high temperature ethanol oxidation". In: *Int. J. Chem. Kinet.* 31.3, pp. 183–220.
- Marinov, N. M. et al. (1998). "Aromatic and polycyclic aromatic hydrocarbon formation in a laminar premixed n-butane flame". In: *Combust. Flame* 114.1-2, pp. 192–213.

## References III



- Mueller, M. A. et al. (1999). "Flow reactor studies and kinetic modeling of the H<sub>2</sub>/O<sub>2</sub> reaction". In: *Int. J. Chem. Kinet.* 31.2, pp. 113–125.
- Pitz, W. J. et al. (2007). "Modeling and experimental investigation of methylcyclohexane ignition in a rapid compression machine". In: *Proc. Combust. Inst.* 31.1, pp. 267–275.
- Pointot, T. and D. Veynante (2005). *Theoretical and numerical combustion*. Philadelphia: RT Edwards, Inc.
- Smith, G. P. et al. (1999). [http://www.me.berkeley.edu/gri\\_mech](http://www.me.berkeley.edu/gri_mech).
- Vincenti, W G and C H Krüger (1965). *Introduction to physical gas dynamics*. Wiley.
- Williams, F. (1994). *Combustion Theory*. New York: Perseus Books.